



Comprehensive Study of Old Open Clusters using multi-wavelength data in the GAIA era

Deeshani Mitra

Supervisor: **Dr. Ashish Raj**

Astrophysics
Summer Fellowship Program-ICSP
SARSTEM, Isophote

Submitted: May, 2018

This Project Report has been submitted in fulfilment of progress requirements for the 12-week research fellowship program at Isophote.

Acknowledgements

With immense pleasure, we thank our Supervisor, Dr. Ashish Raj, for his patience, motivation, and sincere guidance throughout the project. We want to extend our heartiest thanks to Dr. Devendra Bisht for his valuable guidance and encouragement. We are indebted to Ashish Sir and Devendra Sir for their continuous support and guidance during the project.

We are beyond grateful for the Astrophysics Research Fellowship Program, where we learned state-of-the-art research methodologies and built a valuable network. The knowledge and skills gained through this fellowship program will stay with us indefinitely.

Abstract

This study presents a comprehensive analysis of the properties of old open clusters using multi-wavelength data in the GAIA era. Open clusters offer a unique opportunity to study the intricacies of galaxy formation and evolution due to their similar ages and chemical compositions as they are formed from the same molecular clouds. Recent studies have shed light on the internal structures, kinematics, and physical properties of open clusters such as Berkeley 26, Berkeley 45, Berkeley 70, NGC 2266, and Tombaugh 4, providing valuable insights into the formation and evolution of stellar systems. In this study, we will conduct a comprehensive analysis of these clusters, including the determination of age by fitting the theoretical PARSEC isochrone models to the observed CMDs for stars upto G-mag ≤ 20 , metallicity, distance, reddening by fitting ZAMS from Caldwell (1993), estimation of radial density profiles by fitting KING's model, luminosity function and metallicity using GAIA EDR3, 2MASS, and LAMOST data. We will also discuss the probable blue straggler stars (BSS) in these clusters near the Main Sequence Turn Off point (MSTO). Furthermore, we will also determine the mean proper motion and parallaxes associated with these clusters. Our investigation aims to contribute to a deeper understanding of the broader aspects of galaxy formation and evolution, essential to enhance our knowledge of the Milky Way's galactic disk and its intricate evolutionary history.

Contents

1	Introduction	1
1.1	Aims and Objectives	1
2	Background & Literature Overview Of Clusters	3
2.1	Berkeley 26	3
2.2	Berkeley 45	4
2.3	Berkeley 70	5
2.4	NGC 2266	6
2.5	Tombaugh 4	7
3	Methodology	9
3.1	Membership Analysis	9
3.2	Radial Density profile	10
3.3	Reddening	10
3.4	Age, Distance, and Metallicity	11
4	Results for each cluster	12
4.1	Result Berkeley 26	12
4.1.1	Identification of cluster and Membership Analysis	12
4.1.2	Proper Motion Analysis	13
4.1.3	Interstellar reddening	14
4.1.4	Color Magnitude Diagram	16
4.1.5	Isochrone Profile	17
4.1.6	Blue straggler Stars	17
4.2	Result: Berkeley 45	18
4.2.1	Membership Analysis and others	18
4.2.2	RA, DEC, and Proper Motion Analysis	18
4.2.3	Color Magnitude Diagram and other analysis	20

4.2.4	Interstellar Reddening	21
4.2.5	Iochrone Fitting	22
4.2.6	Luminosity Function	23
4.3	Result: NGC 2266	24
4.3.1	Membership Probability:	26
4.3.2	Mean Proper Motion:	32
4.3.3	Distance from Mean Parallax:	32
4.3.4	Radial Density Profile :	33
4.3.5	Reddening:	35
4.3.6	Metallicity:	36
4.3.7	Age-Metallicity Relation:	36
4.3.8	Age and Distance Estimation Through Isochrone Fitting :	37
4.3.9	Blue Straggler Stars (BSS):	40
4.3.10	Luminosity Function :	41
4.4	Result: Berkeley 70	42
4.4.1	Membership Analysis	42
4.4.2	Physical parameters of the cluster	42
4.4.3	Color magnitude diagram	42
4.4.4	Extinction	44
4.4.5	Isochrone fitting	45
4.5	Result: Tombaugh 4	47
4.5.1	Membership Analysis and Others	47
4.5.2	RA, DEC, and Proper Motion analysis	47
4.5.3	Color Magnitude Diagram (CMD)	48
4.5.4	Interstellar Reddening	49
4.5.5	Isochrone fitting	50
4.5.6	Luminosity Function (LF)	50
5	Discussion & Conclusions	53
5.1	Berkeley 26	53
5.2	Berkeley 70	53
5.3	Berkeley 45	53
5.4	Tombaugh 4	54
6	Future Work	55
6.1	Scope 1	55

6.2 Scope 2	55
6.3 Scope 3	55
References	56

List of Figures

2.1	Berkeley 26 from SDSS	3
2.2	Berkeley 45 from SDSS	4
2.3	Berkeley 70 from SDSS	5
2.4	NGC 2266 from SDSS	6
2.5	Tombaugh 4 from SDSS	7
4.1	RA-DEC of Berkeley 26	13
4.2	Membership probability of cluster members and field stars of Berkeley 26 . .	13
4.3	Vector Point diagram of Berkeley 26	14
4.4	Parallax of all the stars of Berkeley 26	14
4.5	Parallax of the cluster the stars of Berkeley 26	15
4.6	Gaussian fitting for proper motion in RA of Berkeley 26	15
4.7	Gaussian fitting for proper motion in RA of Berkeley 26	15
4.8	Gaussian fitting for proper motion in RA of Berkeley 26	16
4.9	Gaussian fitting for proper motion in RA of Berkeley 26	16
4.10	Isochrone Profile Berkeley 26	17
4.11	G-magnitude vs. Probabilities of Berkeley 45	18
4.12	G-magnitude vs. Parallax of Berkeley 45	19
4.13	Proper motion components vs. the number of counts of Berkeley 45	19
4.14	Vector Point Diagram of Berkeley 45	20
4.15	CMD of Berkeley 45	21
4.16	CMD of Berkeley 45 with GAIA EDR3 and GAIA DR2 data (Cantat-Gaudin and Anders (2020))	21
4.17	Color-color diagram for Berkeley 45, using 2MASS data	22
4.18	Isochrone fitted CMD of Berkeley 45	23
4.19	Luminosity function of Berkeley 45	23

4.20 (Proper motion distribution of member stars, (G, G BP-RP) CMDs with membership probability higher than 80 percent for the cluster stars only. The clustered red part represents the cluster center in Ra vs. Dec plot.	24
4.21 Vector Point Diagram of NGC 2266: On the left panel, we have, All stars, on the next panel; cluster with probable members, and on the right panel, only field stars	25
4.22 Color Magnitude Diagram (G BP-RP vs. Gmag) : The left panel has all stars, the middle panel has only probable members with more than 80 percent probability, and the right panel has field stars	25
4.23 a) Geometric errors in proper motions and parallax with G magnitude, b) Photometric errors in Gaia bands (G, BP, RP) with G magnitude.	26
4.24 Errors in magnitudes J, H, K with J magnitude	26
4.25 Membership Probability as a function of G magnitude , where red circles denote member stars with membership probability of more than 80 percent, and black circles are below 80 percent.	27
4.26 Distribution for the membership probabilities of the stars in the NGC 2266 region, the stars above 80 percent are considered member stars, where most member stars have a high probability of 1.0, which means they are located at the center of the cluster.	27
4.27 Right Ascension vs Declination: Red dots are member stars, and black dots are field stars.	28
4.28 Proper Motion Right Ascension vs. Declination: , on the left panel, we have our members obtained: 554 above 80 percent, on the right, we have Cantat-Gaudin Members obtained: 194 above 80 percent	29
4.29 Color Magnitude Diagram (Gbp-rp vs. Gmag):	29
4.30 Color-Magnitude diagram of NGC 2266 after DBSCAN method.	30
4.31 Proper motion of stars.	30
4.32 RA vs Dec of stars.	30
4.33 Color-Magnitude diagram of NGC 2266 after UPMASK method.	31
4.34 Proper motion of stars.	31
4.35 RA vs Dec of stars.	31
4.36 Proper Motion Histograms in R.A. and Dec of the cluster NGC 2266 using GMM. The Gaussian fit to the center provides the mean values shown in each panel.	32

4.37 Profiles of stellar counts across the region of NGC 2266. a) The Gaussian fits have been applied to the histograms. The center of symmetry about the peaks of R.A. and Dec is taken as the cluster's center. b) The probable member stars with positive parallax are denoted by red in this apparent magnitude vs. parallax graph stars.	33
4.38 Profiles of stellar counts across the region of NGC 2266. The Gaussian fits have been applied to the histograms. The center of symmetry about the peaks of R.A. and Dec is taken as the cluster's center.	34
4.39 Surface Density Distribution of the cluster NGC 2266, where errors are determined using sampling statistics $1 / \sqrt{N}$, where N is the number of stars used in density estimation at that point. The smooth line represents the fitted King's profile, and dashed line represents background density, and the dotted line represents the errors in background density. The Poisson errors are so low in range (0.11– 0.18) that they are not visible in the plot.	35
4.40 Color Color Diagram: The red solid line is the zams taken from Caldwell data, where the dotted line is the same zams shifted in such a way that it displaces the solid line.	36
4.41 The log age 9.05 best-fitted isochrone with different z values to show the importance of correct metallicity.	37
4.42 All the stars here are probable member stars above 80 percent probability. The curves are isochrones of log ages 8.95, 9.05, and 9.15. The red stars denote 194 probable members matched with Cantat-Gaudin members with above 80 percent membership probability.	38
4.43 Isochrone fittings with different log ages.	39
4.44 The suspected blue straggler stars with blue dots in CMD.	40
4.45 Luminosity function of NGC 2266 using members.	41
4.46 An initial cut of 0.3 mas/yr is used to separate the possible cluster stars from the field stars	43
4.47 Membership probabilities of Berkeley 70	43
4.48 Proper motion distribution of Berkeley 70	44
4.49 Distribution of parallaxes of the cluster Berkeley 70. Here the negative (unphysical) parallaxes are excluded.	44
4.50 Color magnitude diagram for Berkeley 70 with all stars having membership probability larger than 50% (right) and the comparison to the members from a catalog of Cantat-Gaudin (left). The color bar on the right indicates the membership probability.	45

4.51 Color-color diagram for Berkeley 70 from 2MASS data. Calwell ZAMS is fitted to the data to estimate the extinction.	45
4.52 Example of the grid of Padova isochrones used to fit the age for Berkeley 70 (right) and the best-fitted isochrones used for age estimation (left)	46
4.53 G-magnitude vs. Probability of Tombaugh 4	47
4.54 G-magnitude vs Parallax for Tombaugh 4	47
4.55 Proper motion components vs. the number of counts of Tombaugh 4	48
4.56 Vector Point Diagram of Tombaugh 4	48
4.57 CMD of Tombaugh 4	49
4.58 Cantat-Gaudin Catalogue(2020) CMD comparison with observed CMD of Tombaugh 4	49
4.59 Color-color diagram for Tombaugh 4, using 2MASS data	50
4.60 Isochrone fitted CMD of Tombaugh 4	51
4.61 Luminosity function of Tombaugh 4	52

List of Tables

5.1	Comparison of the present study with literature for Berkeley 45	54
5.2	Comparison of the present study with literature for Tombaugh 4	54

Introduction

1.1 | Aims and Objectives

Open Clusters(OCs) are astronomical laboratories that preserve the history of the Galactic disk; this includes tracing the galaxy's chemical abundance and dynamical evolution. OCs are fundamental objects since they constrain galaxy evolution theories. With the assistance of the GAIA mission, more than 2000 star clusters have been studied via their spectroscopic, photometric, and astrometric data, revolutionizing our understanding of the Milky Way as OCs form and evolve along the Milky Way plane. Moreover, clean CMDs and more accurate estimation of ages have been obtained in recent times due to the availability of more precise data on parallaxes, proper motions, metallicities, other structural, kinematical, and dynamical properties, such as orbit, eccentricity, angular momenta, total energy, and 3D Galactic velocities of OCs(Fu et al. (2022)). These objects are of utmost importance while studying the galactic structure because they are formed from the same molecular cloud with gas and dust that measures thousands of times the sun's mass. Therefore, the chemical composition of their stellar components is similar, as well as their age. They can comprise around a few tens to a few thousand stars which are gravitationally bound in the cluster. The ages of OCs can range from a few hundred million to a few billion years. Sometimes, the possibility of two OCs forming from the same molecular cloud is also possible, which results in a binary cluster. The most probable site for finding such structures is the galaxy's spiral arm, where the density of open clusters is high (Subramaniam et al. (1995)).

The old open clusters we aim to study deeply in this project are **Berkeley 26, Berkeley 45, Berkeley 70, NGC 2266, and Tombaugh 4**. We have chosen these particular clusters since they haven't been examined in depth, and many parameters involve certain discrepancies.

Berkeley 26, also known as Biurakan 12, is a very old open cluster estimated at roughly 4.5 Gyr in Monoceros. It is a very distant cluster at 7.8 kpc and is highly reddened, E(VI) = 0.80. The Galactic longitude= 207.694, and the Galactic latitude = 2.346 per the WEBDA database. It is a Trumpler class III 1m (moderately dense) with an angular diameter of 4 arcmin. To our knowledge, there are only four previously existing studies on this cluster: (Tadross

(2010)), (Hasegawa et al. (2008b)), (Carrera (2012)), and (Piatti et al. (2010b)) in which the last three studies have identical parameter estimation but specific differences remain, indicating a potential difference in the underlying data or methodology.

Berkeley 70, which belongs to the Perseus arm, has many blue straggler stars. The Galactic longitude = is 166.894, and the Galactic latitude = is 3.580 with a distance of 4158 pc as per the WEBDA database. It has a solar metallicity of $[Fe/H] = 0.01 \pm 0.14$ dex (Carrera (2012)) (using V and I magnitudes). It has a roughly estimated age of 4 Gyr. Reddening obtained for this cluster is $E(BV) = 0.48 \pm 0.10$ mag with a distance modulus of 13.1. To our best knowledge, only two other studies exist in UBV photometry exist on this cluster: (Ann et al. (2002b)) and (Hasegawa et al. (2004)) in addition to the previously mentioned study.

NGC 2266, also known as Melotte 50, has an age of roughly 1.2 Gyr (Reddy et al. (2013)). The Galactic longitude= 187.790 and Galactic latitude= 10.294 as per the WEBDA database. The metallicity of this cluster is derived to be $[Fe/H]=-0.38\pm0.07$ (Carrera (2012)) with only V magnitudes. A distance of 3100 pc has been estimated to the cluster and reddening, $E(B-V) = 0.10$ (Monteiro et al. (2010)). There have been several studies on this cluster; we aim to do its analysis with the latest GAIA EDR3 data.

Berkeley 45 is present in a rich galactic field. The Galactic longitude is 50.040, and the Galactic latitude is 1.145, taken from the WEBDA database. The log(age) has been estimated to be 8.5-8.6 (Subramaniam et al. (2010)). The cluster is located at a distance of 2350 parsec. A reddening of $E(B-V) = 0.82$ mag was determined by Tadross (2010) but Subramaniam et al. (2010) found $E(B-V) = 1.4$ mag. To our knowledge, these two studies have been mentioned in this cluster. The V vs. (BV) CMD suggests the presence of asterism.

Tombaugh 4 is an unstudied compact and rich cluster with Galactic longitude = 134.207 and Galactic latitude = 1.082, as per the WEBDA database. It has $\log(\text{age}) = 8.6-8.7$ and is present at a distance of 3.85 kpc (Subramaniam et al. (2010)). In the CCD BV survey by Maciejewski and Niedzielski (2007), $\log(\text{age}) = 9$ has been estimated for the cluster with $E(B-V) = 1.01$ mag. It is located at a distance of 2.17 kpc, as per the study. To our best knowledge, only these two studies exist for this old open cluster.

Background & Literature Overview Of Clusters

2.1 | Berkeley 26

Berkeley 26, called Biurakan 12 or C0647+08, is a very old and poorly studied cluster in Monoceros. Over the years, some studies have been done on Berkeley 26 to define fundamental parameters such as distance, age, stellar population, metallicity, etc. Various photometry, astrometry, and spectroscopy methods have been used for these studies.

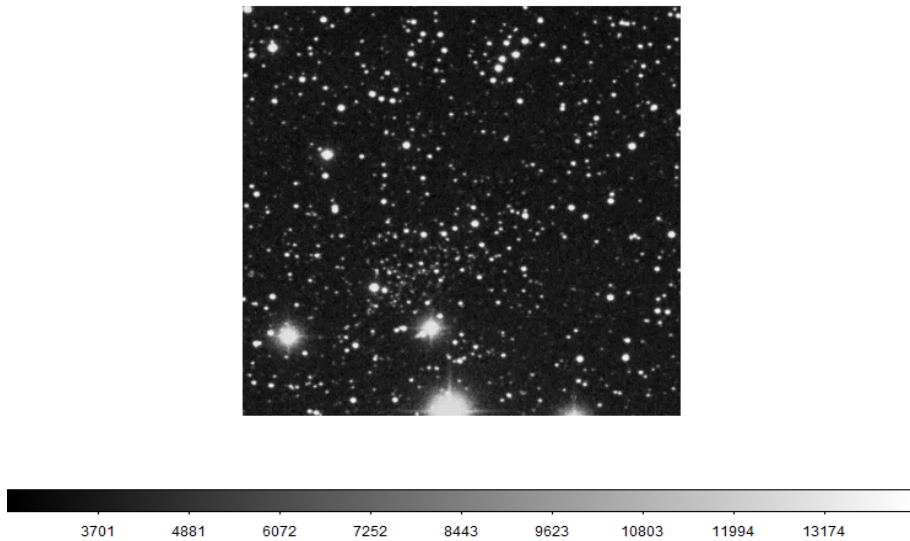


Figure 2.1: Berkeley 26 from SDSS

In the literature, till now, only 4 studies have been done for this cluster to our knowledge. **Hasegawa et al. (2008a)** and **Piatti et al. (2010a)** have used BVI spectroscopy while **Carrera (2012)** used medium-resolution spectra ($R = 8000$) in the infrared CaT region and **Tadross (2008)** used JHK photometry from 2mass. **Hasegawa et al. (2008a)**, **Piatti et al. (2010a)** and **Tadross (2008)** have derived the age, reddening, distance, and metallicity utilizing isochrone fitting. **Hasegawa et al. (2008a)** and **Piatti et al. (2010a)** derived the age of 4.5 Gyrs and 4 Gyrs

respectively, while **Tadross (2008)** derived a much younger age of 0.6 yrs, even the reddening value derived by **Tadross (2008)** is relatively lower compared to **Hasegawa et al. (2008a)** and **Piatti et al. (2010a)**. As noted by **Piatti et al. (2010a)**, poor quality of data and selected cluster members may be the reason for such differences in the results. **Carrera (2012)** derived a metallicity of 0.43 ± 0.20 and 0.35 ± 0.17 dex , **Piatti et al. (2010a)** derived a value of -0.7dex while **Hasegawa et al. (2008a)** assumed the value of -0.35.

In conclusion, Berkeley 26 is an old open cluster with high reddening, making it a challenging target for study. Overall, the extensive research on Berkeley 26 has provided valuable insights into the formation and evolution of open clusters and their role in the broader context of galaxy formation and evolution.

2.2 | Berkeley 45

Berkeley 45, located in the Aquila constellation in the first quadrant of the galaxy, is an old open cluster present in a rich galactic field. It is a Trumpler class II2p cluster, i.e., it features a central area with moderate concentration. As mentioned earlier, this constellation has been subject to minimal study by the scientific community. The positional coordinates for the cluster are 'ra' = 19:19:12 and 'dec' = +15:43:00. The cluster CMD does not show a sharp MSTO, and literature has reported the presence of asterism (**Subramaniam et al. (2010)**). There are only two known studies on this cluster in which **Tadross (2010)** used 2MASS photometry to investigate the cluster's different properties, whereas **Subramaniam et al. (2010)** used BV I CCD photometry. A brief overview of their studies has been discussed ahead.

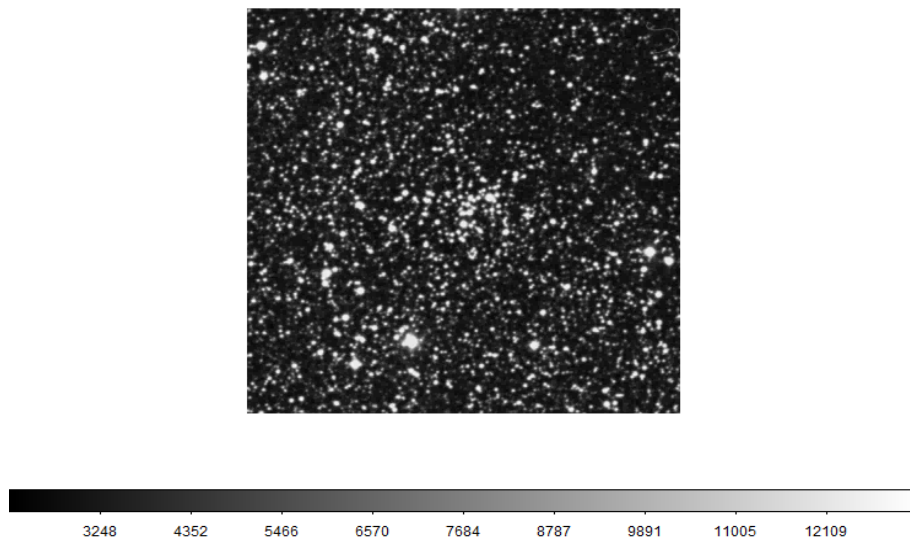


Figure 2.2: Berkeley 45 from SDSS

Subramaniam et al. (2010) predicted a younger age for the cluster in range of $\log(\text{age}) = 8.5\text{-}8.6$. They obtained a distance of 2350 pc which is within range of the previous study, and a high reddening value, $E(\text{BV}) = 1.4$ mag. They also mentioned a distance modulus of 16.2. Tadross (2010) predicted a $\log(\text{age})$ of 8.77 or 0.6 Gyr. The distance was estimated to be 2300 pc. The reddening value obtained was $E(\text{B-V}) = 0.82$ mag and cluster radii of 3.5'.

We aim to study the cluster in GAIA photometry for the first time and obtain the parameters such as age, distance, metallicity, reddening, and others to add to the previously existing studies for a further comprehensive understanding of the cluster's properties. We will also use 2MASS data to obtain reddening by fitting ZAMS from Caldwell's (1993) intrinsic colors. This project aims to advance our knowledge of old open clusters in the Milky Way and provide insights into the features and characteristics of Berkeley 45.

2.3 | Berkeley 70

Berkeley 70 is a very poorly studied open cluster. Little could be found in the literature about this cluster except for the paper from Ann et al. (2002a) and Hasegawa et al. (2008a).

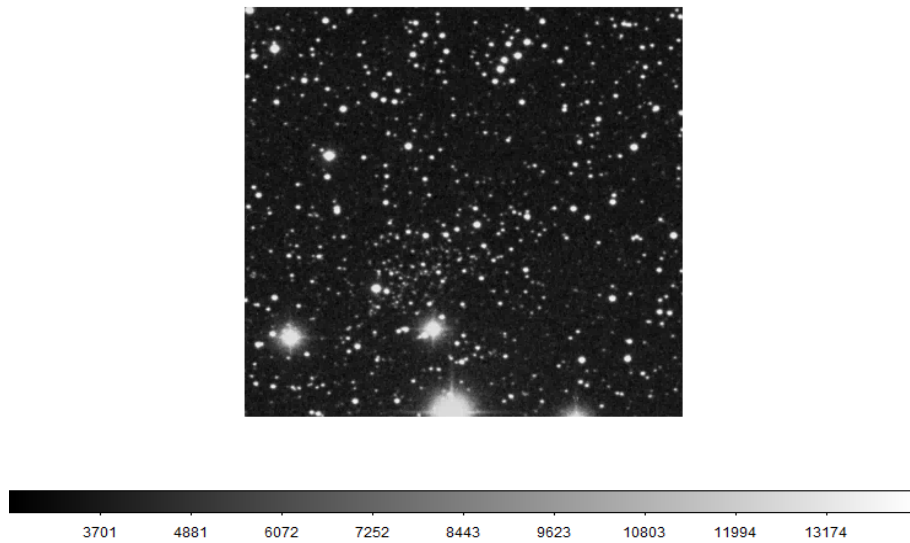


Figure 2.3: Berkeley 70 from SDSS

This cluster seems to have several blue stragglers, making it a very interesting candidate cluster to study the origin of these stars in detail. The reddening value reported by Ann et al. (2002a) for this cluster is 0.48 ± 0.10 while the $\log(\text{age})$ is reported as 9.6 ± 0.1 . The mean distance is reported to be 4158 pc. However, they didn't use bias corrections while reporting the distances for the cluster. Hence these values might vary after bias correction. Interestingly, this

cluster contains a distinct, well-developed giant branch, indicating an evolved cluster. There is no binarity analysis found for this cluster as well. Membership probabilities are found for 450 stars from Cantat-Gaudin (2020), which summarizes the available literature on this cluster so far.

2.4 | NGC 2266

NGC 2266, also known as Melotte 50 and Herschel (81), named after an astronomer, is an open cluster in the constellation of Gemini. It was discovered by a German-British astronomer named William Herschel on December 7, 1785.

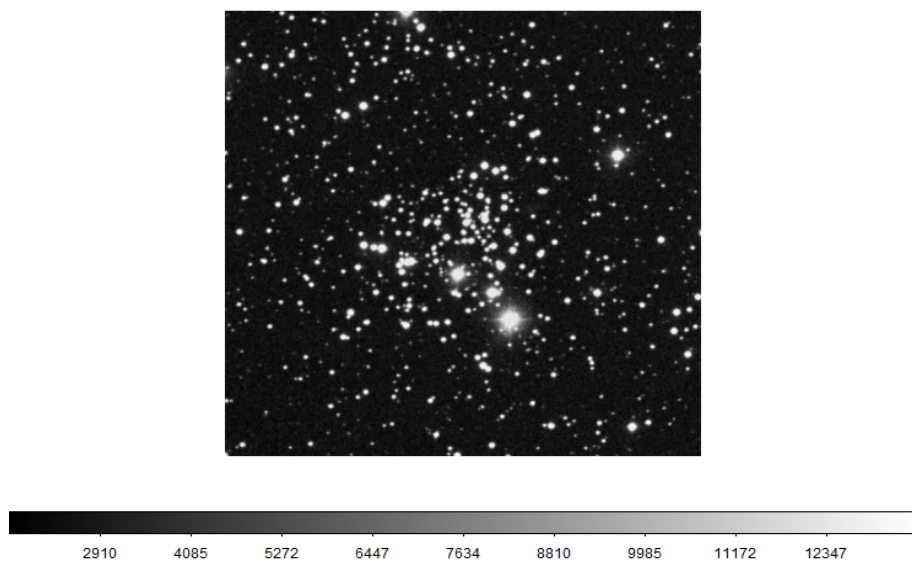


Figure 2.4: NGC 2266 from SDSS

The position of this cluster in the sky is Right ascension: 06h 43m 20.2s, Declination: +26° 59' 06", having an apparent size of 5.2 arc minutes, apparent magnitude 9.5 and is known to have a distance of 3469 parsecs. This is a compact star cluster known to have many stars on the main sequence and is popularly known for its 11 red giants, which have been listed in many research papers. Two-three blue straggler stars were also reported for NGC 2266 by a research paper. Also, having a set of 12 binary stars, this open cluster has been a point of interest since the 90s among various scientists. Most blue stars in the cluster core are "hydrogen-burning stars," but many stars left this evolutionary stage because their central hydrogen is exhausted, and now they burn their hydrogen in a shell around the stellar nucleus and appear as bright red giants. The brightest stars in the image are the foreground stars, which do not belong to the cluster population.

2.5 | Tombaugh 4

Tombaugh 4 is a rich and compact old open cluster in the northern constellation Cassiopeia. The positional coordinates for the cluster from the WEBDA database are 'ra' = 02 29 10 and 'dec' = +61 47 42.

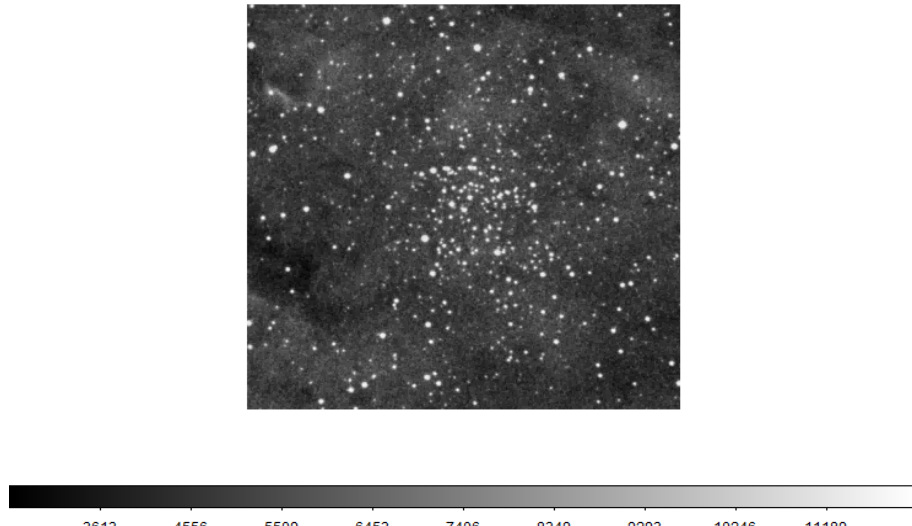


Figure 2.5: Tombaugh 4 from SDSS

In this study, GAIA photometry will be used to analyze the cluster in detail with stars up to G-mag ≤ 20 . A brief overview of the present literature is discussed ahead. Two existing studies on this cluster, where **Subramaniam et al. (2010)** presented the BVI CCD photometry, found a dense cluster core. The CMD obtained in their study has a well-defined main sequence with a sharp MSTO point. They found that the cluster has a moderately young age with a $\log(\text{age})$ range of 8.6-8.7 and is located at a distance of 3.85 kpc. They also estimated the radial density profiles and obtained a half-power radius and effective radius of 1.3 and 2.5 arcmin, respectively. The reddening values obtained are $E(B-V) = 1.25$ mag and a distance modulus of 16.8.

Maciejewski and Niedzielski (2007) also used BV wide-field CCD photometry to study the cluster and obtained a $\log(\text{age}) = 9$ which is slightly higher than the previous study. The ages, reddenings, and distances obtained use the solar metallicity range for isochrone fitting. The reddening values derived are $E(B-V) = 1.01$ which is identical to the previous study. They obtained distance modulus values as $(M - m) = 14.81$ and estimated a distance of 2.17 kpc to the cluster. The structural parameters obtained for the cluster are $f_0(\text{central density}) = 12.91 \text{ stars}/\text{arcmin}^2$, $f(\text{bg})$, i.e., the density of the stellar background in the field = $1.62 \text{ stars}/\text{arcmin}^2$, $r(\text{core}) = 1.1'$ and $r(\text{lim}) = 5.6'$.

This present study aims to use the GAIA EDR3 data along with 2MASS data and any other relevant datasets to supplement the research to obtain the above-mentioned parameters. The metallicity values have not been determined in the literature so far. Therefore, an attempt to extract the metallicity value will be made. The membership analysis will be done via pyUPMASK, built over UPMASK. We will obtain the reddening values through JHK magnitudes of the 2MASS data and use reference intrinsic colors from CALDWELL DATA(1993).

Methodology

3.1 | Membership Analysis

The initial step to examine star clusters involves determining the membership stars to remove the contaminating field stars present in the foreground and background of cluster members. This can be done using proper motions, parallaxes, and based on other parameters as well. Disentangling these two classes of elements of members from nonmembers (i.e., field stars) is known as "decontamination." The effectiveness of cluster star membership analysis depends on the techniques and restrictions applied to the data. Multiple factors contribute to the quality of the membership analysis. Certain methods like Gaussian Mixture Model(GMM) and, DBSCAN, pyUPMASK, among others, have been utilized in previous studies.

In the report, we have used two methods for membership analyses: pyUPMASK and GMM. One such method used for membership determination is pyUPMASK (**Pera et al. (2021)**), which is an unsupervised clustering technique that is built upon the original UPMASK (Unsupervised Photometric Membership Assignment in Stellar Clusters algorithm) package. Unlike other previously used methods, the word 'unsupervised' refers to the fact that no prior selection of comparison field stars is taken as a reference model. This method is particularly useful for obtaining precise results for the GAIA EDR3 data used in this study based on 'proper motion' data.

Another method used to determine membership probability is GMM, an unsupervised clustering similar to the maximum likelihood (ML) method popularly used for membership determination. The GMM model is useful where the clusters have an "elliptical" shape and is used to represent Normally distributed sub-populations within an overall population. Cleanly separates the stars, which are members of the open clusters. This model is a category of the probabilistic model which states that all the generated data points are derived from a mixture of finite Gaussian distributions.

We aim to derive probabilities above 70%, 80%, 90% based on the dataset of each cluster. These cluster stars can be used to calculate the parameters discussed ahead.

3.2 | Radial Density profile

The first step in obtaining the RDP of the cluster is to determine the center. To do so, a Gaussian function can be fitted to the distribution of the stars, and the point of maximum number density is assumed as the (**Bisht et al. (2021)**). The center estimation is followed by constructing an RDP by taking concentric circles around the center with annular regions in arcmin, and stellar densities are calculated for each region (taken as an ith zone). Therefore, stellar density becomes:

$$\rho_i = \frac{N_i}{A_i}$$

where N_i is the number of stars in that ith zone, and A_i is the area of the zone (Bisht et al. (2021)).

This is followed by fitting of **King (1962)** model to the RDP, given as:

$$f(r) = f_b + \frac{f_0}{1 + (r/r_c)^2}$$

where r_c , f_b , and f_0 are core radius, background density, and central stellar density.

The background and central density have the units of *stars/arcmin*², and the core radius is in *arcmin*. The cluster's radius and other structural parameters for the clusters Berkeley 26, Berkeley 45, Berkeley 70, NGC 2266, and Tombaugh 4 have been discussed in the results section of the respective clusters.

3.3 | Reddening

To calculate interstellar reddening E(B-V), we will use the near-infrared JHKs photometric data from 2MASS data, i.e., the 2-Micron All Sky Survey. The J-H vs. J-K Color-Color Diagrams (CCDs) of the observed cluster will be fitted with the solar metallicity ZAMS taken from **Caldwell et al. (1993)**. The JHK color error cut-off value will be 0.15 for better observations. While estimating the reddening, we will also check if the ratio of E(J-H) and E(J-K) is in good agreement with the value of 0.55 as given by **Cardelli et al. (1989)**. The obtained values of E(J-H) and E(J-K) will be used to calculate E(B-V) using the relations given by **Fiorucci and Munari (2003)**:

$$E(J - K) = 0.48 \times E(B - V)$$

$$E(J - H) = 0.309 \times E(B - V)$$

The obtained interstellar reddening from JHK colors will be compared with the existing values in the previous studies of the respective clusters Berkeley 26, Berkeley 45, Berkeley 70, NGC 2266, and Tombaugh 4.

3.4 | Age, Distance, and Metallicity

The Color Magnitude Diagrams are extremely essential tools to study open clusters and determine their parameters such as age, distance, metallicity, and reddening, which can further help us understand the evolution of our galaxy. They indicate the evolutionary stages of the cluster stars, i.e., we can identify the main-sequence, giant stars, and the white dwarfs in addition to blue straggler stars in a few cases.

To observe CMD with GAIA EDR3 data of the clusters Berkeley 26, Berkeley 45, Berkeley 70, NGC 2266, and Tombaugh 4, we plotted the G-magnitude ($<=20$) and G(BP-RP) colors. Further, to determine the age, distance, and metallicity, we fitted PARSEC theoretical isochrones with the CMD tool by **Marigo et al. (2017)** (<http://stev.oapd.inaf.it/cgi-bin/cmd>) corresponding to the particular $\log(\text{age})$ and a metal fraction (z) of the concerned cluster.

The obtained $\log(\text{age})$ will be compared with the available studies to check if it is consistent with the literature. This will help us investigate the reliability of our age estimates.

4

Results for each cluster

In this chapter, we are providing all estimated parameters for our used clusters in this project. The results of each parameter of five open clusters are given below in this table.

Cluster Parameters							
Cluster Name	Member Count	Mean PM ra dec [mas/yr]	Radial Density P rlim rc fbg f0	Redden E(B-V)	z val	Age (Gyr)	Dist. (pc)
Berkeley 26	cell						
Berkeley 45	699	1.534 , 4.484	-	0.80	0.01	9	-
NGC 2266	554	-0.483, -0.238	6' , 1.6' , 0 ,	0.17	0.004	0.957	3311
Berkeley 70	cell5	cell6					
Tombaugh 4	484	0.987 , 0.109	-	1.012	0.009	9.2	3775.15

In these sections, we will study all the results with all parameters listed in the table for every cluster in detail.

4.1 | Result Berkeley 26

4.1.1 | Identification of cluster and Membership Analysis

We have used multidimensional GAIA DR3 data for the astrometric analysis of Berkeley 26. Complete data up to $G = 20$ mags is only considered. For membership probability, we have used the pyUPMASK method. This cluster has a distinct nearby cluster Berkeley 27, due to which data with a search radius of 10 arcmin was taken, giving 4604 stars; 355 stars were obtained for probability above 0.9.

Right Ascension vs. Declination plot where the cluster of stars can be seen as marked with a '+' in black as the center. The central coordinates were 102.5625000 and 5.7300000 degrees for Ra and Dec, respectively. After taking the membership probability, we can see that the cluster members are highlighted in red. We have taken data only in the black-marked circle with a radius of 0.8 degrees to filter out some data due to many field stars.

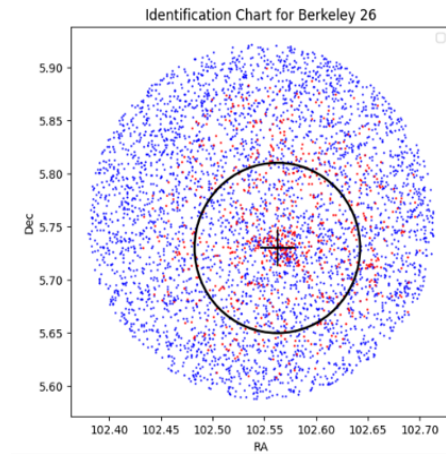


Figure 4.1: RA-DEC of Berkeley 26

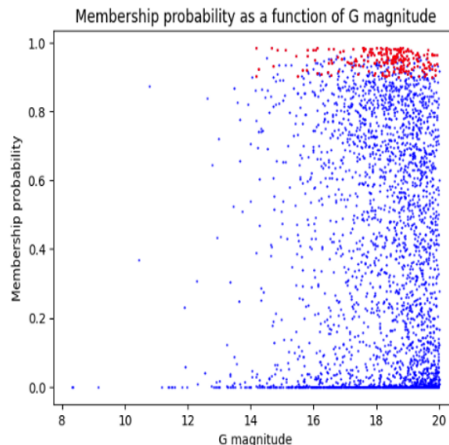


Figure 4.2: Membership probability of cluster members and field stars of Berkeley 26

G-magnitude vs. probability data for cluster members (red) and field stars (black) was obtained from the above data. For further studies, cluster members with a probability above 90 % (red) are only considered with G up to 20 mag.

This specific approach allows the researchers to concentrate on the most likely members of the cluster, ensuring a more accurate and refined investigation. By filtering out stars with lower probabilities and those with higher magnitudes, they can effectively narrow their analysis to a subset more likely to represent genuine cluster members, minimizing the inclusion of field stars or other spurious data points.

4.1.2 | Proper Motion Analysis

Proper motion graphs of PMRA and PMDEC as vector point diagrams (VPDs) were plotted to see how cluster members and field stars are distributed in space.

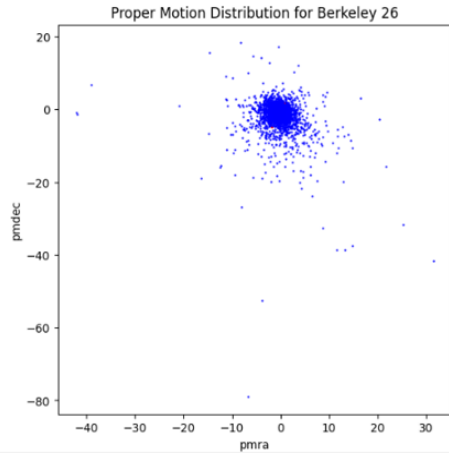


Figure 4.3: Vector Point diagram of Berkeley 26

Parallax vs. G- the magnitude of the data with cluster members(red) above probability 90 percent and field stars(black), their mean parallax value was calculated and estimated to 0.19 ± 0.22 mas and 0.32 ± 0.37 mas respectively

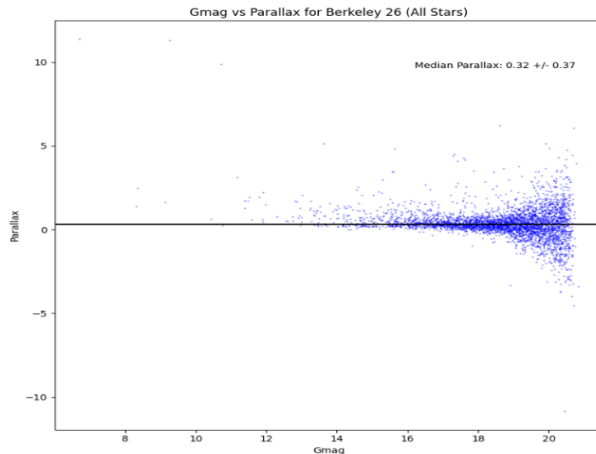


Figure 4.4: Parallax of all the stars of Berkeley 26

Gaussian fitting was performed to get the mean values of PMRA and PMDEC, which are approximately 0.01 ± 0.36 and 0.21 ± 0.57 mas/yr, respectively. This gives the location of maximum stellar density or the cluster.

4.1.3 | Interstellar reddening

Interstellar reddening was obtained for Berkeley 26 with a value of 0.43 ± 0.02 and the ratio of $E(J-H)/J-K) = 0.56$; these values agree with the values obtained by Tadross (2008).

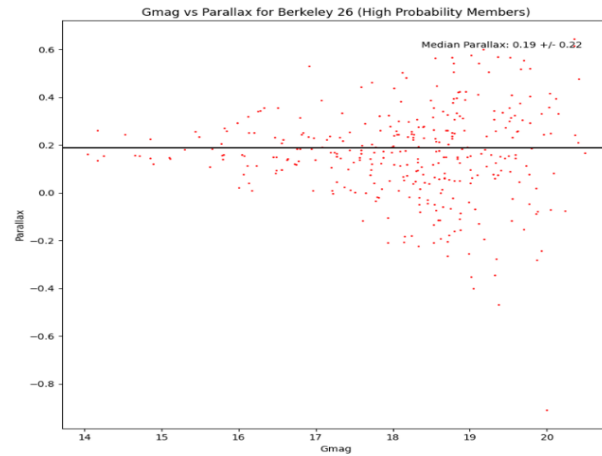


Figure 4.5: Parallax of the cluster the stars of Berkeley 26

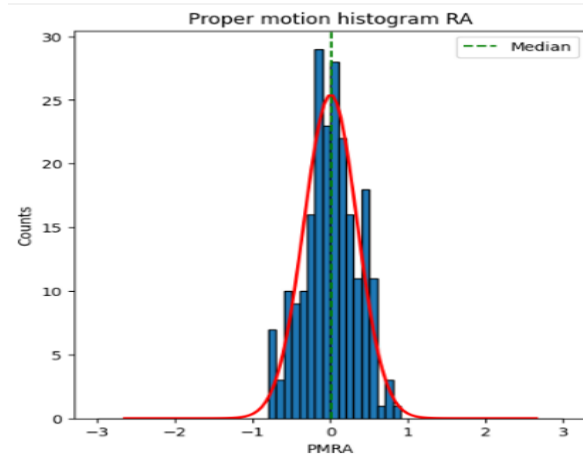


Figure 4.6: Gaussian fitting for proper motion in RA of Berkeley 26

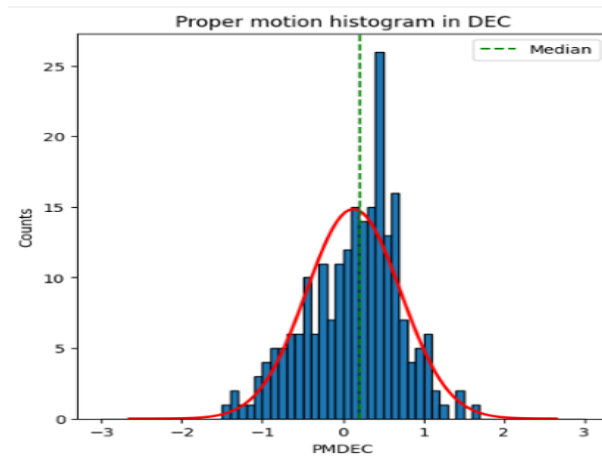


Figure 4.7: Gaussian fitting for proper motion in RA of Berkeley 26

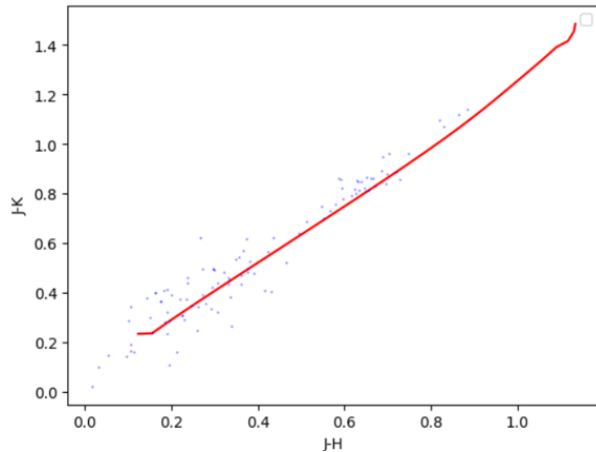


Figure 4.8: Gaussian fitting for proper motion in RA of Berkeley 26

4.1.4 | Color Magnitude Diagram

Color Magnitude Diagram (CMD) is an effective tool for determining the age, distance, and reddening using some theoretical fitting models of the cluster; for this cluster, the CMD for cluster members (red), Field stars (blue), and both together were plotted. As can be seen, the cluster members show a good main sequence stars line, and some scattering is observed near the giant stars as well.

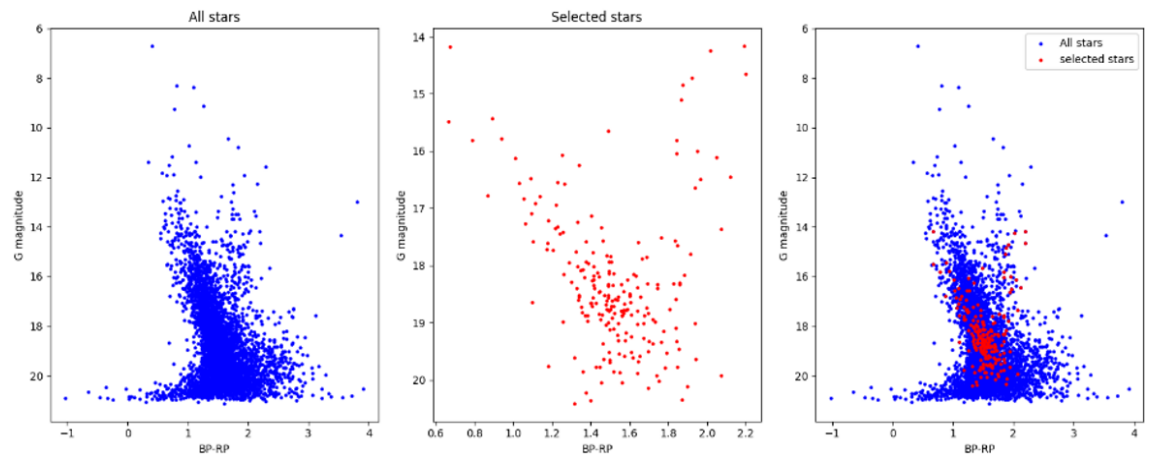


Figure 4.9: Gaussian fitting for proper motion in RA of Berkeley 26

To conduct more in-depth studies, the researchers have focused solely on cluster members whose probability of being part of the cluster exceeds 90 %. Additionally, the selection criterion for this subgroup is that their G-magnitude does not exceed 20 mags. In other words, only those stars with a high likelihood of belonging to the cluster and brightness (as indicated by the G-magnitude) below 20 mags are included in the further analysis.

4.1.5 | Isochrone Profile

We estimated the log(age) for Berkeley 26 and found it to be 9.55, assuming a metal fraction of 0.75, corresponding to solar metallicity. To validate our estimation, we compared it with PARSEC isochrones of log(age) values 9.65, 9.55, and 9.45, 2.5-4 Gyrs, which agrees with the literature. Our analysis indicates that the isochrone with log(age) = 9.55 best fits the observed CMD (Color-Magnitude Diagram) of Berkeley 26.

In the accompanying figure, the blue solid dots represent potential blue straggler stars (BSS), typically located near the Main Sequence Turn Off point. Among the four potential blue straggler stars displayed, one particular star stands out with coordinates RA= 102.5625000 and DEC=5.7300000, and its existence has been verified by **Piatti et al. (2010a)**.

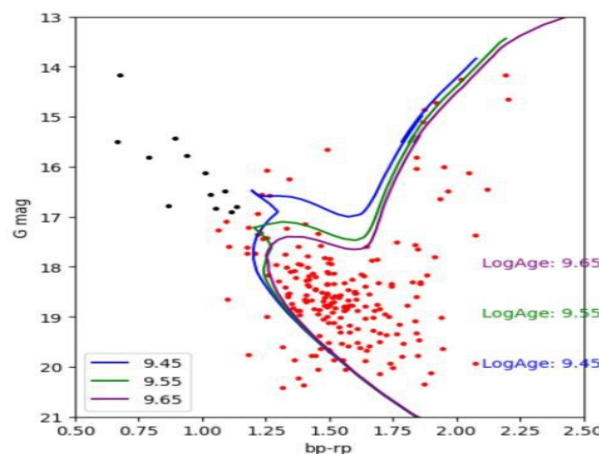


Figure 4.10: Isochrone Profile Berkeley 26

4.1.6 | Blue straggler Stars

A blue straggler is a type of star that is more luminous and bluer than expected. Typically identified in a stellar cluster, they have a higher effective temperature than the main sequence turnoff point for the cluster, where ordinary stars begin to evolve towards the red giant branch. The blue dotted lines are denoted as BSS stars in figure 4.10. These stars are seen above $G \geq 16$ mags.

4.2 | Result: Berkeley 45

4.2.1 | Membership Analysis and others

Using the GAIA EDR3 data, we analyzed the results for the old open cluster Berkeley 45 with pyUPMASK. As previously mentioned, Berkeley 45 is present in a rich galactic field, i.e., a densely populated galaxy area. The GAIA EDR3 data with a search radius of 10 arcmin yielded a significant number of 21954 stars. After doing the pyUPMASK analysis, built over the original UPMASK package, we isolated 699 stars with a probability above 0.9.

The G-magnitude vs. the probabilities plot of cluster members (in red) and field stars (in black) shows the magnitudes over which the stars in the clusters are situated. We will only use these cluster members for subsequent studies unless otherwise specified.

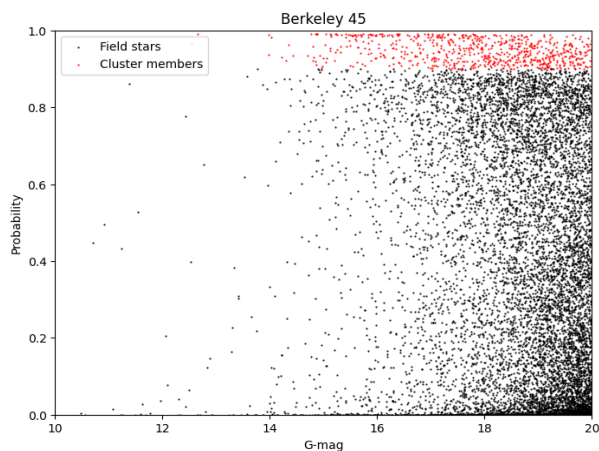


Figure 4.11: G-magnitude vs. Probabilities of Berkeley 45

The parallax (apparent shift in the position of stars) and G-magnitude plot has also been given where the cluster members above 50 % probability are represented as solid circles and vice-versa for the field stars. The parallax measurements have been plotted after applying an offset to correct certain biased values. The mean parallax value obtained for Berkeley 45 is 0.304 ± 0.008 mas.

4.2.2 | RA, DEC, and Proper Motion Analysis

The first essential step is obtaining the location of maximum stellar density; the cluster center obtained is RA = 289.78, DEC = 15.71. The proper motion data was also analyzed along with its two components, i.e., 'pmra' and 'pmdec.' The mean values for proper motion and its components obtained with Gaussian fitting are: Mean proper motion in RA = -1.534 ± 0.015 mas/yr, Mean proper motion in DEC: -4.484 ± 0.018 mas/yr. Further, the VPD, i.e., the Vector Point Diagram, has been plotted, a plot of the pmra vs. pmdec where each star in a cluster is

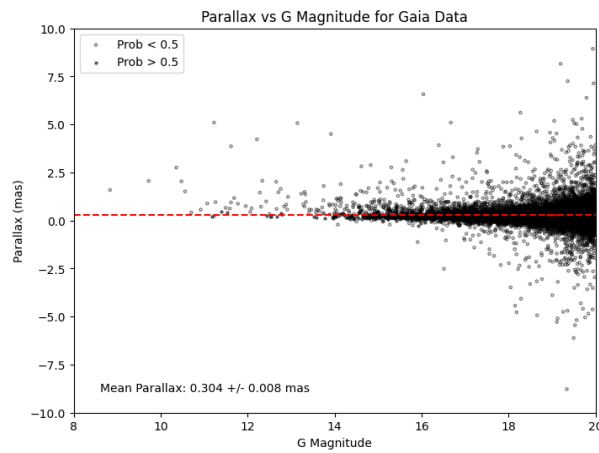


Figure 4.12: G-magnitude vs. Parallax of Berkeley 45

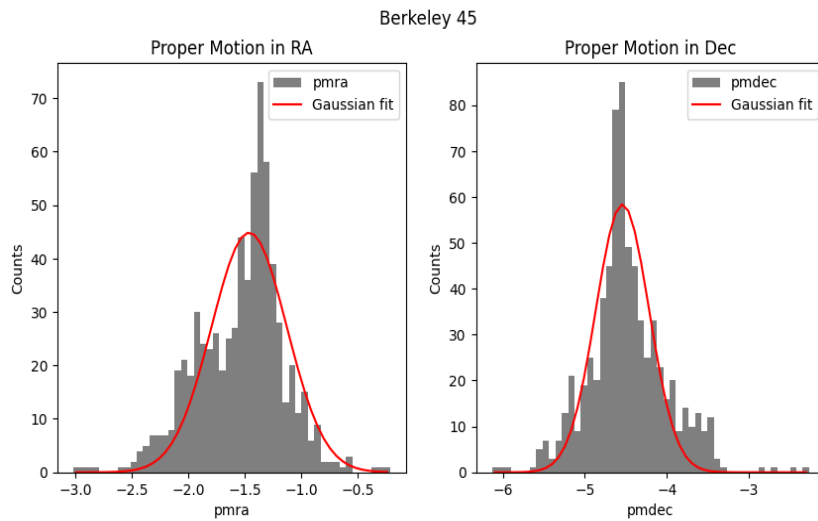


Figure 4.13: Proper motion components vs. the number of counts of Berkeley 45

represented as a point. Previous studies used it to identify cluster members using all stars, i.e., the field and cluster stars.

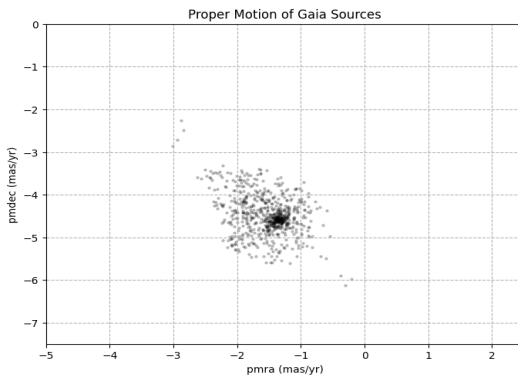


Figure 4.14: Vector Point Diagram of Berkeley 45

4.2.3 | Color Magnitude Diagram and other analysis

The Color Magnitude Diagram is a powerful fundamental tool for understanding the evolutionary stages of the stars in the clusters. It is a plot of magnitudes vs. colors, in this case, G vs. G(bp-rp), where the cut-off value applied for G-magnitude is ≤ 20 . We can easily identify the main-sequence stars, the giant branch stars, and in some cases, blue stragglers near the MSTO, i.e., the Main Sequence Turn Off point. By studying the CMD of clusters, we can identify other properties such as age, metallicity, and reddening. The CMD obtained for Berkeley 45 is given below. The comparison between CMD of field stars, cluster stars, and field stars is visible as the region containing all stars and field stars is heavily crowded. Whereas the CMD of cluster stars is clean.

An interesting thing to notice in this case is another pattern emerging on the right side of the CMD. This pattern has also been observed in other photometric studies of Berkeley 45. It might be a potential asterism, as mentioned by Subramaniam et al. (2010), i.e., the stars in this pattern are not essentially bound gravitationally to the cluster.

In addition to studying the CMD using traditional methods, we also attempted to use the Gaussian Mixture Model (GMM) and Density-Based Spatial Clustering of Applications with Noise (DBSCAN) methods to obtain the CMD for Berkeley 45 and determine its membership probability. However, we found that the GMM method did not give a clean CMD, while the DBSCAN method produced a good CMD but did not provide a membership probability. These results suggest that while machine learning methods may be useful in some cases, they may not always provide the desired results when studying star clusters. It is important to carefully evaluate the methods and interpret the results to ensure they are accurate and reliable.

A comparison between the Cantat-Gaudin and Anders (2020) catalog has also been shown with the CMD obtained in this study for Berkeley 45 with GAIA EDR3 data. Cantat-Gaudin and Anders (2020) used G-magnitudes of stars ≤ 18 using GAIA DR2 data and visual inspection methods utilizing the proper motion and parallax distributions of cluster components.

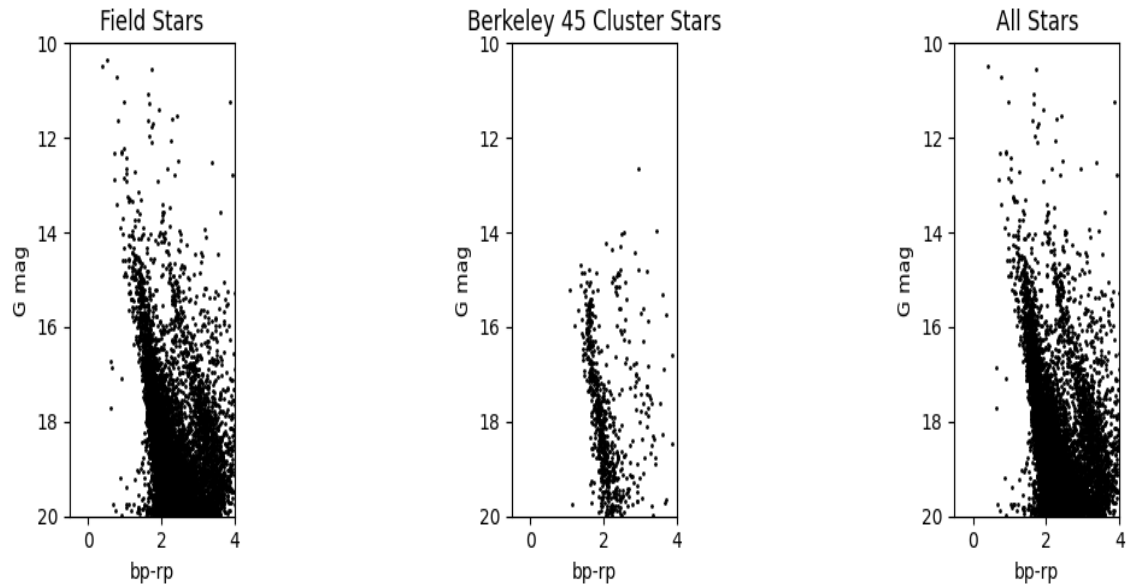


Figure 4.15: CMD of Berkeley 45

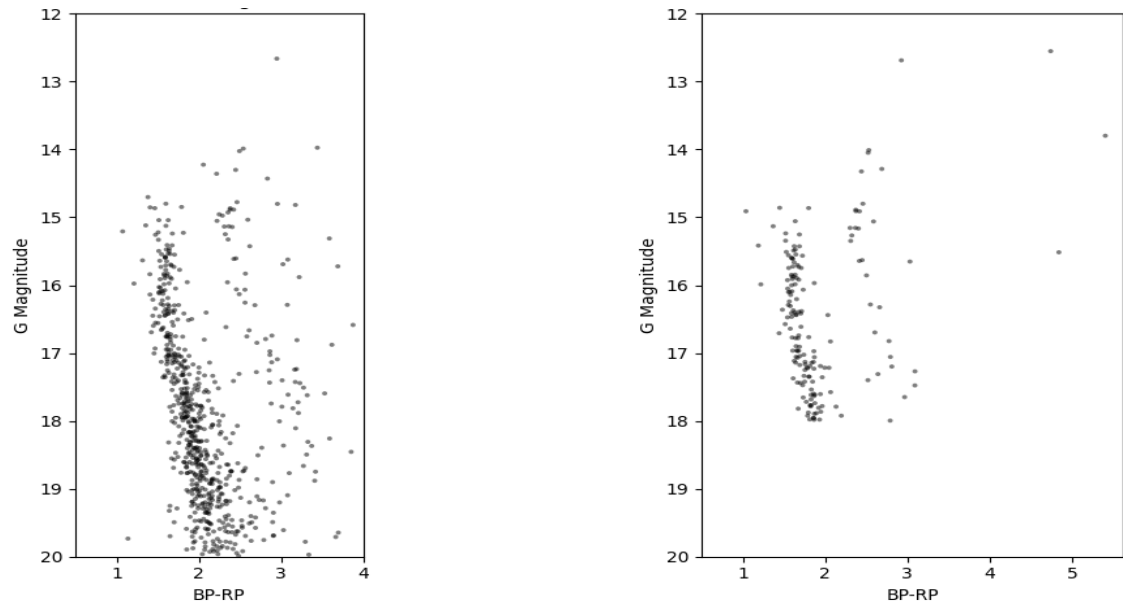


Figure 4.16: CMD of Berkeley 45 with GAIA EDR3 and GAIA DR2 data (Cantat-Gaudin and Anders (2020))

4.2.4 | Interstellar Reddening

The interstellar reddening i.r. $E(B-V)$ obtained for Berkeley 45 in this study agrees with the one obtained by Tadross(2008), i.e., 0.80. The ratio of $E(J-H)$ and $E(J-K) = 0.55$, which is in good agreement with Cardelli et al. (1989).

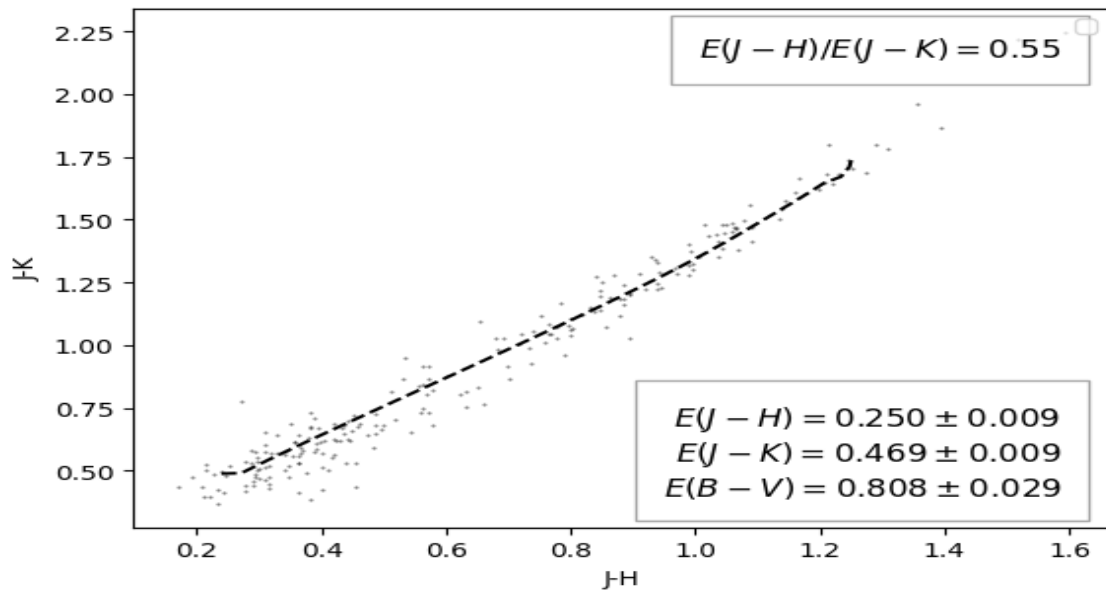


Figure 4.17: Color-color diagram for Berkeley 45, using 2MASS data

4.2.5 | Isochrone Fitting

We estimated the $\log(\text{age})$ of Berkeley 45 = 9 with a metal fraction = 0.01 which corresponds to solar metallicity. In the figure below, the comparison with PARSEC isochrones of $\log(\text{age})$ = 8.90, 8.95, and 9 are shown, and we can conclude that $\log(\text{age})$ = 9 isochrone is the best fit to the observed CMD of Berkeley 45. The blue solid dots are the potential blue straggler stars (BSS) generally spotted near the Main Sequence Turn Off point. Out of the four potential blue straggler stars shown, one with RA= 289.771285 and DEC= 15.707554 has been confirmed by **Jadhav and Subramaniam (2021)**.

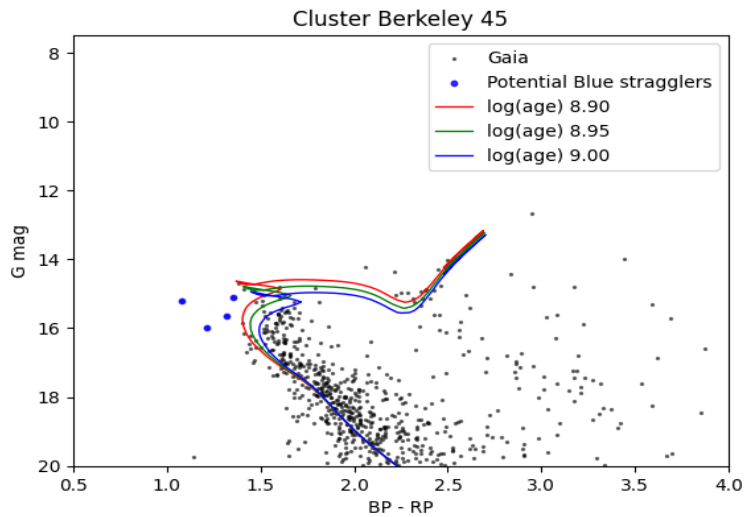


Figure 4.18: Isochrone fitted CMD of Berkeley 45

4.2.6 | Luminosity Function

For the dynamical study of the cluster, the distance modulus is used to obtain the absolute magnitudes of the main sequence stars. We have plotted the histograms of LF with intervals of 1.0 mag. The LF continues to rise to $M(g) = 4$ for the cluster. The mean luminosity function value obtained = 3.296 mag.

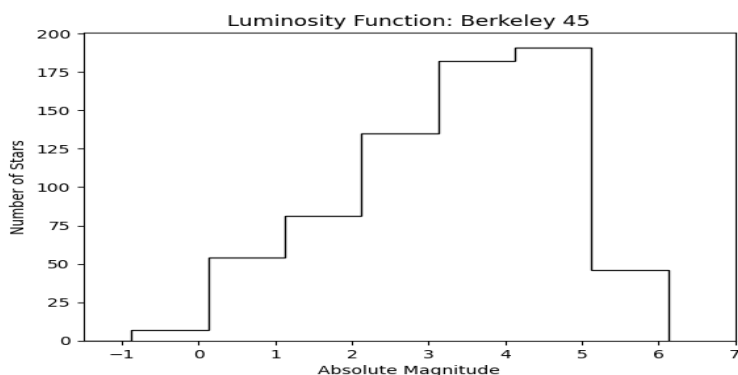


Figure 4.19: Luminosity function of Berkeley 45

4.3 | Result: NGC 2266

In this work, the study of geometric and photometric analyses on the various parameters of the open cluster NGC 2266, taken from Gaia Early Data Release (EDR3) to derive the fundamental structural and kinematical parameters, is performed. The data has included G magnitude and other parameters of member stars with more than 18 percent mag under 80 percent cutoff. The spatial and geometric parameters, i.e., radial density, cluster center: 100.832, 26.976, size of the cluster: 6', distance from parallax is estimated using Ra, Dec, Parallax of the probable member stars. Also, the photometric parameters like age: 0.957 Gyr, reddening: $E(B-V)=0.17$, distance from J, K, H magnitudes, G BP-RP, and G magnitudes were also determined to be 3533 and 3311pc. The cluster members were separated from the field stars using two unsupervised clustering methods: GMM and UPMASK.

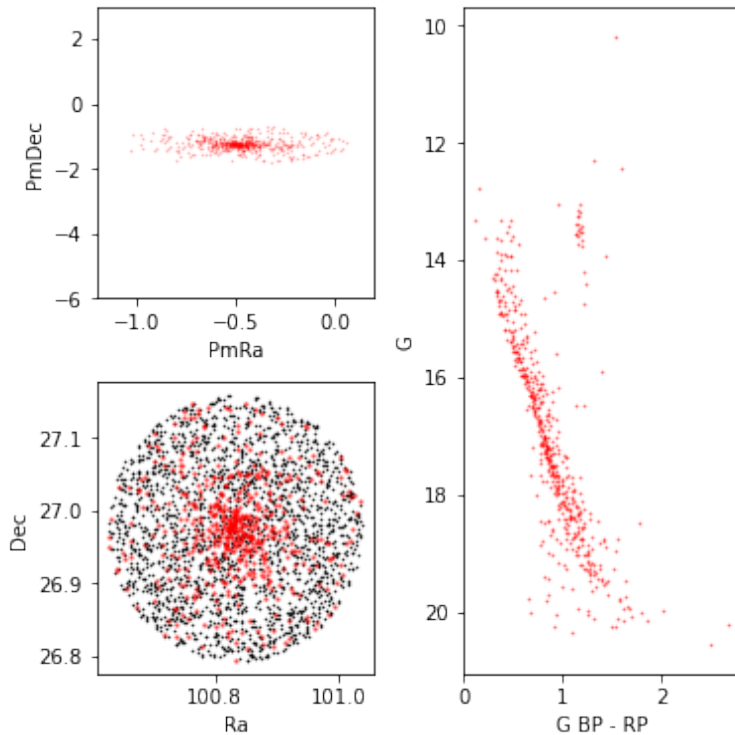


Figure 4.20: **(Proper motion distribution of member stars, (G, G BP-RP) CMDs with membership probability higher than 80 percent for the cluster stars only. The clustered red part represents the cluster center in Ra vs. Dec plot.**

In an open cluster, the stars are loosely bound to gravitational force, originate from the same source have the same vectorial movements in the sky (reference Yontan, 23 March). These stars are expected to have proper motions tightly distributed around the mean proper motion value, as shown in the figure below.

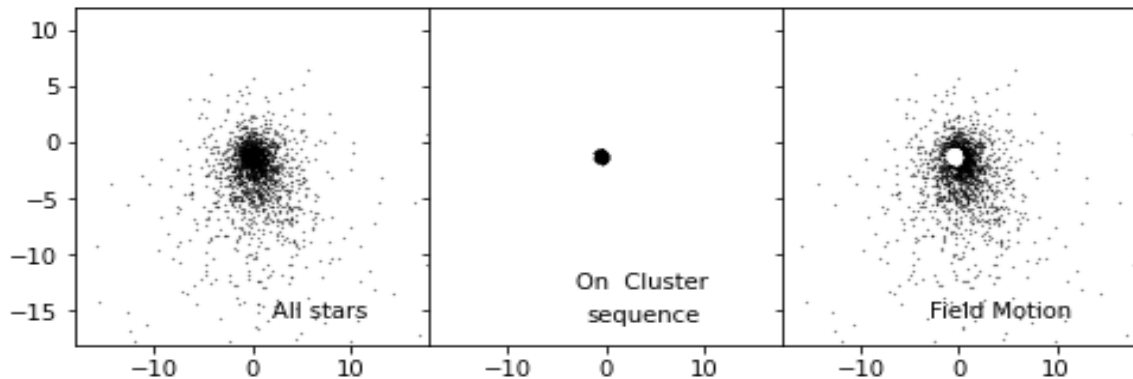


Figure 4.21: **Vector Point Diagram of NGC 2266:** On the left panel, we have, All stars, on the next panel; cluster with probable members, and on the right panel, only field stars

A star is considered a cluster member if it lies inside the circle in a Vector Point Diagram and has a parallax value within 3 sigmas from the mean cluster parallax, which is discussed in detail in the next section about Mean Parallax.

A Color Magnitude Diagram is an important aspect of studying open clusters. It gives visual information on the main sequence, turn-off of the stars, and blue straggler stars which have moved out of the trajectory of the main sequence.

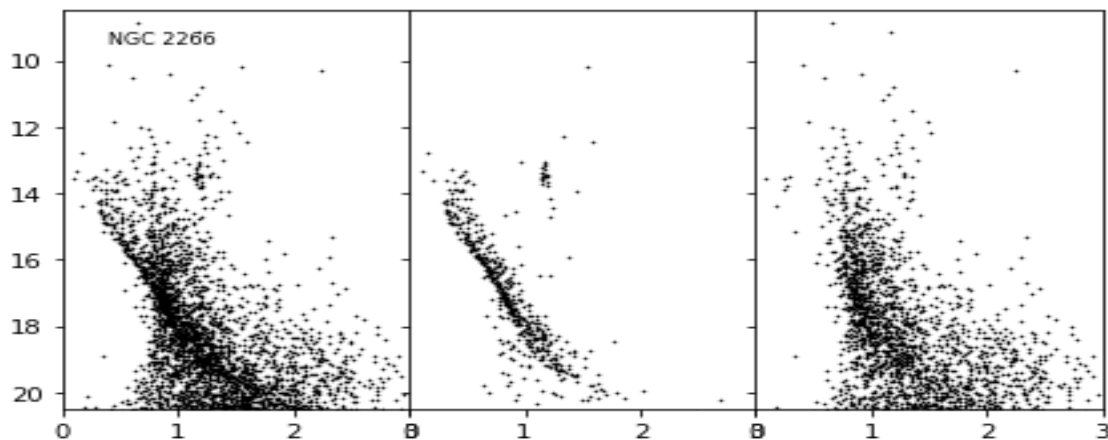


Figure 4.22: **Color Magnitude Diagram (G BP-RP vs. Gmag) :** The left panel has all stars, the middle panel has only probable members with more than 80 percent probability, and the right panel has field stars

Parameteric Errors: Most stars are so distant or faint that sometimes uncertainties of their parameters are large. Photometric distances additionally use the G magnitude and BP-RP color from the EDR3. To know about the errors in these parameters, J, H, K vs. J and G BP-RP vS. G magnitude is plotted as follows:

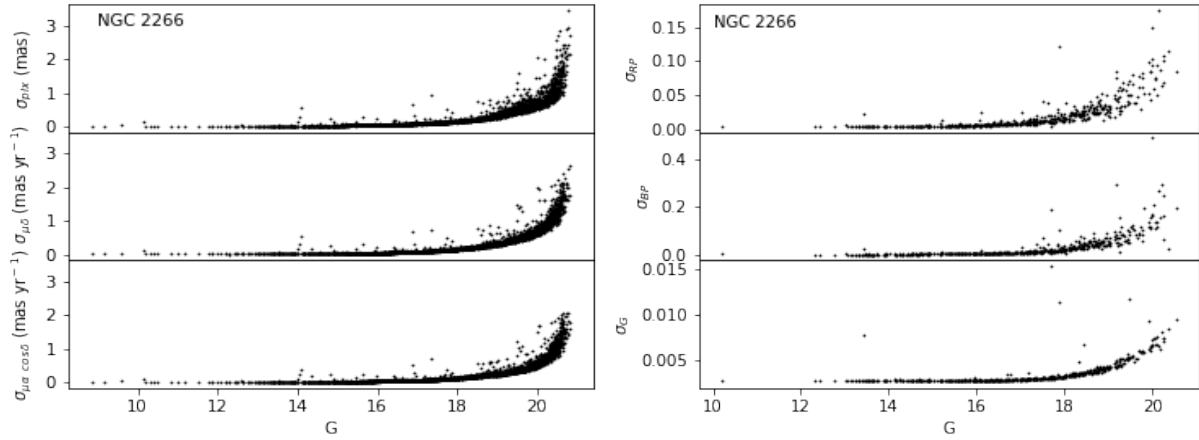


Figure 4.23: a) Geometric errors in proper motions and parallax with G magnitude, b) Photometric errors in Gaia bands (G, BP, RP) with G magnitude.

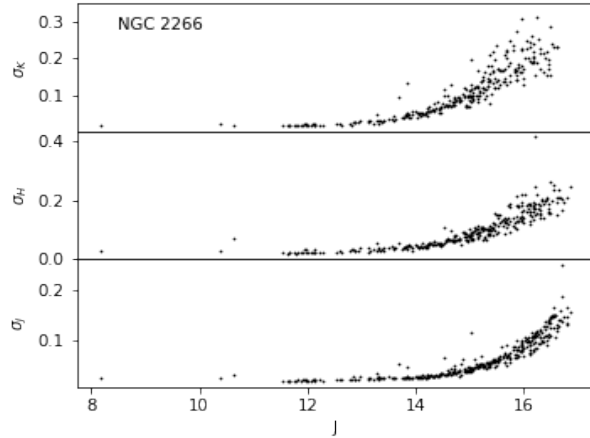


Figure 4.24: Errors in magnitudes J, H, K with J magnitude

Methods used: DBSCAN, GMM, UPMASK

Tools: Topcat, GITHUB, Python scripting

4.3.1 | Membership Probability:

Determination of the correct member of the stars with the cluster is the foremost important step in studying an open cluster.

The distribution of member stars and the field stars in an open cluster is different as member stars are found in groups: dense, and the field stars are dispersed. Therefore, these dense stars are likely to be the member stars clustered together, having more density towards the center, whereas the low-density field stars are placed away from the center.

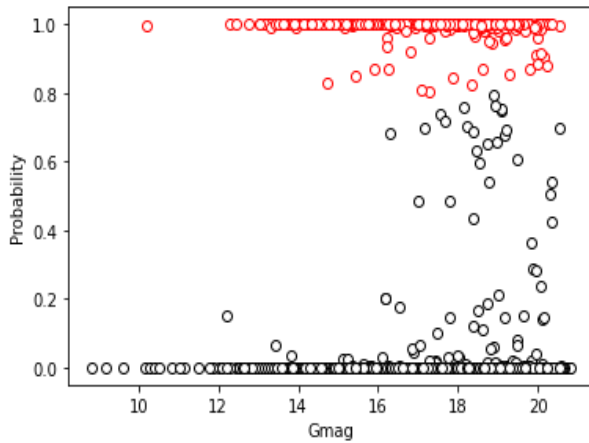


Figure 4.25: **Membership Probability as a function of G magnitude**, where red circles denote member stars with membership probability of more than 80 percent, and black circles are below 80 percent.

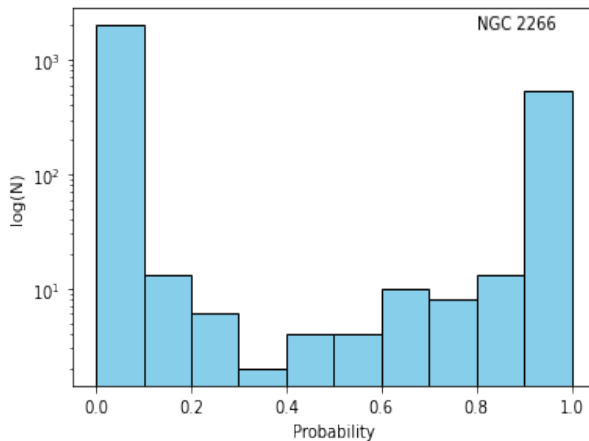


Figure 4.26: Distribution for the membership probabilities of the stars in the NGC 2266 region, the stars above 80 percent are considered member stars, where most member stars have a high probability of 1.0, which means they are located at the center of the cluster.

Initially, K-means and DBSCAN methods were also tried to obtain the membership and clustering properties of this open cluster, but the K-means algorithm did not seem suitable for clustering an open cluster with a spherical shape where the density has to be maximum at the center, and DBSCAN provided clean main sequence, but it doesn't provide the list of probabilities.

To identify the likely members in the study, Unsupervised Photometric Membership methods with iterative processes: GMM and UPMASK, were successfully applied to obtain the member stars.

4.3.1.1 | GMM:

GMM Gaussian Mixture Model is a clustering method where the shape of the data set is expected to be spherical; the method used here consists of soft-clustering. First, the five astrometric parameters from the data set for our cluster were used, namely: **Ra**, **Dec**, **Parallax**, **PmRa**, **PmDec** with normalization. The predict() method was used to find probabilities, followed by GMM being fitted into the data frame, and nearly 500 iterations were processed to obtain the correct group of member stars. Then, these probabilities were filtered out on an 80 percent cutoff. 554 members with probability ≥ 80 were obtained out of 3103 stars, which can be seen in the figure below.

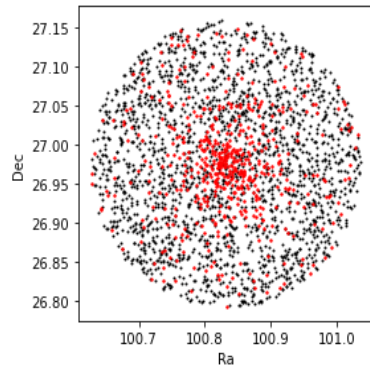


Figure 4.27: **Right Ascension vs Declination:** Red dots are member stars, and black dots are field stars.

4.3.1.2 | Comparison between Cantat-Gaudin Members and Member stars obtained from GMM

A. Proper Motion Right Ascension vs. Declination:

In a proper motion plane, the property of the distribution of stars has been very useful in determining the membership probability, as visible in Figure (4.13). Using Gaia EDR3, 554 members were detected, whereas Cantat Gaudin detected only 194 members above 80 percent probability using EDR2 for the same radius search.

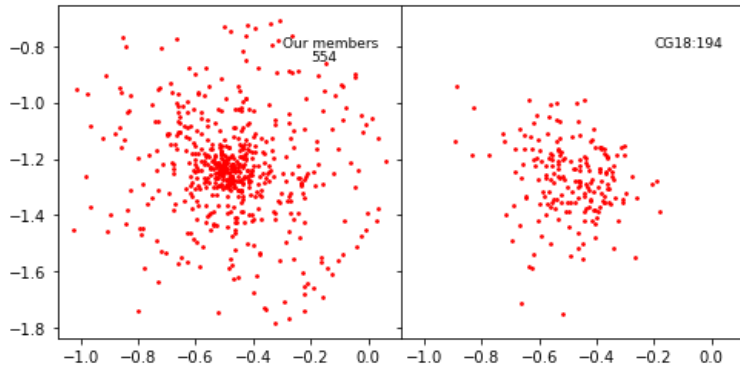


Figure 4.28: Proper Motion Right Ascension vs. Declination: on the left panel, we have our members obtained: 554 above 80 percent, on the right, we have Cantat-Gaudin Members obtained: 194 above 80 percent

B. Color Magnitude Diagram (GBp-Rp) vs. Gmag: The CMD of a stellar cluster is an effective tool for estimating its age, distance, and reddening. These are also helpful in separating member stars and field stars in cluster main sequences. Above 80 percent membership probability, all Cantat-Gaudin members were matched with the members obtained from GMM. It is more evident from the CMD that EDR3 and the method used for membership probability provided more information about the main sequence than Cantat Gaudin, as visible in the figure below.

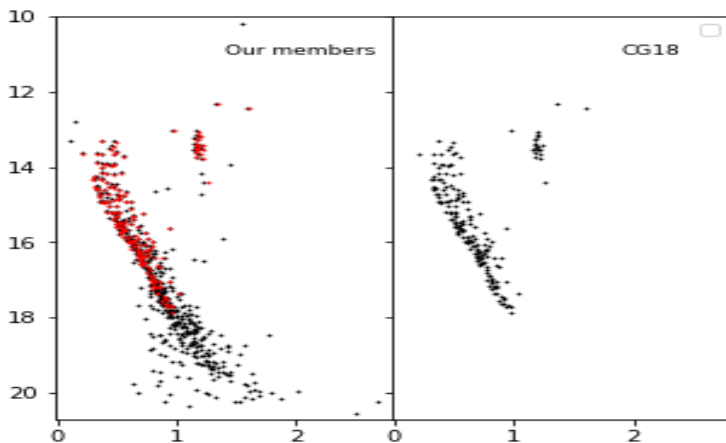


Figure 4.29: Color Magnitude Diagram (Gbp-rp vs. Gmag):
Our members vs. Cantat-Gaudin for above 80 percent membership probability, where red dots on the left panel are matched Cantat-Gaudin members with our members mainly on the main-sequence.

4.3.1.3 | DBSCAN :

DBSCAN is a density-based clustering algorithm. It accepts two input parameters: the number of minimum samples and the search radius. We iterate over different values of minimum samples and search radius to get expected results and a clean CMD plot. For the clustering of data for NGC 2266, we use the following parameters: Minimum Samples = 14; and the Search Radius = 0.48

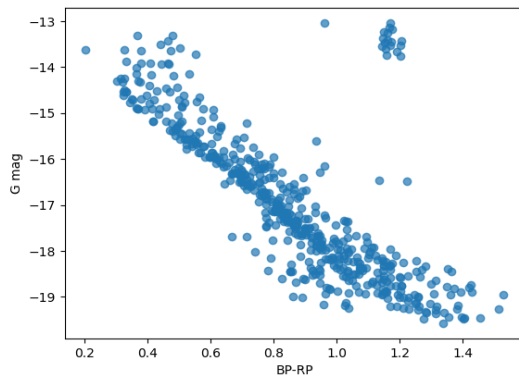


Figure 4.30: Color-Magnitude diagram of NGC 2266 after DBSCAN method.

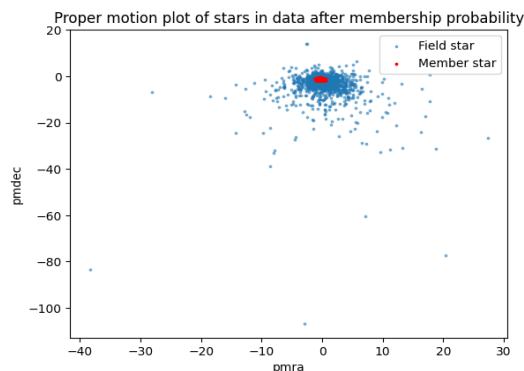


Figure 4.31: Proper motion of stars.

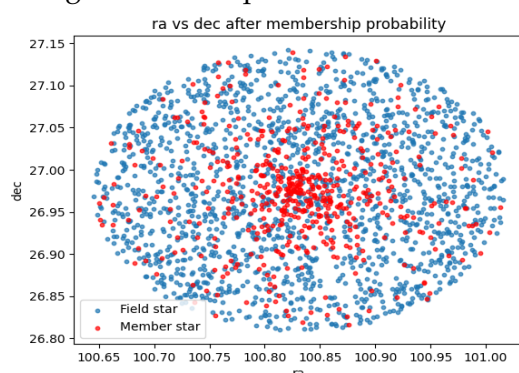


Figure 4.32: RA vs Dec of stars.

4.3.1.4 | UPMASK method:

pyUPMASK is an unsupervised clustering method built on the UPMASK package to identify member stars in a star cluster. The number of member stars identified for NGC 2266 was 428, with a membership probability of 0.8.

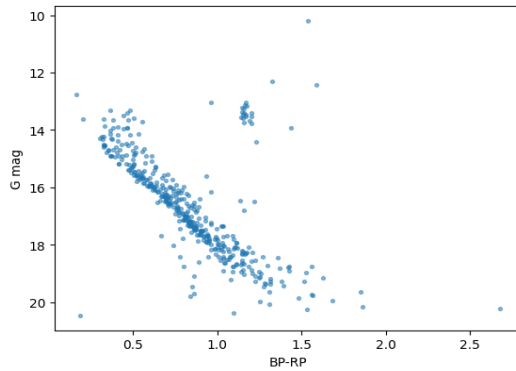


Figure 4.33: Color-Magnitude diagram of NGC 2266 after UPMASK method.

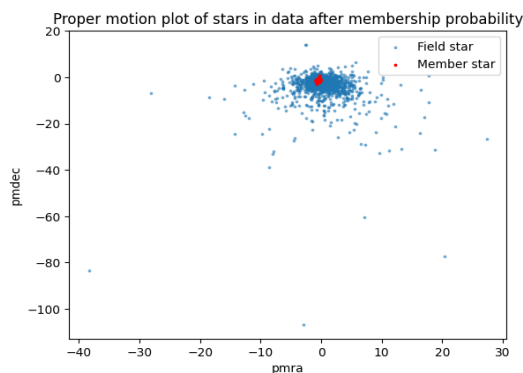


Figure 4.34: Proper motion of stars.

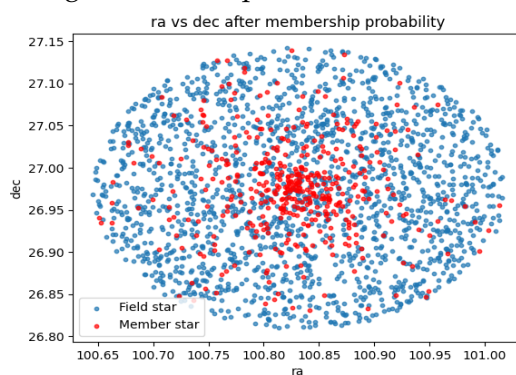


Figure 4.35: RA vs Dec of stars.

4.3.2 | Mean Proper Motion:

It is required to have precise information about the proper motions to differentiate between the member stars from field stars. The kinematical data from the Gaia EDR3 catalog separated cluster stars from field stars.

For the mean estimation of mean proper motion, only probable cluster members were included visible in the VPDs and CMDs, and the one-dimensional Gaussian function was fitted on the constructed histograms. The mean proper motions in directions R.A. and dec. were determined from the peaks of the Gaussian distribution by using GMM and UPMASK.

The PmRa mean and PmDec mean Histogram obtained with Gaussian fitting are:

Mean PmRa: - 0.483 +-0.012 mas/yr

Mean PmDec: -1.238 +- 0.012 mas/yr

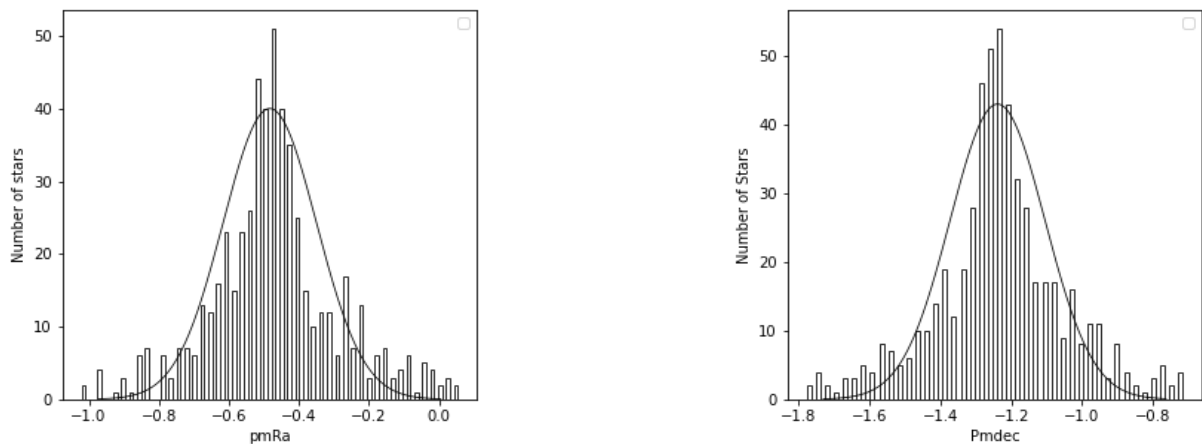


Figure 4.36: Proper Motion Histograms in R.A. and Dec of the cluster NGC 2266 using GMM. The Gaussian fit to the center provides the mean values shown in each panel.

4.3.3 | Distance from Mean Parallax:

The astrometric parameter 'parallax' determines the distance of the open clusters. The Gaia EDR3 parallax for these clusters has been corrected for this cluster by using offset as described in Lindergren et al.,2013. The parallax values of probable member stars were used to construct a histogram, and one-dimensional Gaussian was fitted over it to obtain the mean value of parallax.

Mean Parallax : 0.0253 +- 0.007 mas/yr

In the second figure, the apparent magnitude vs. parallax was plotted in the graph; where the

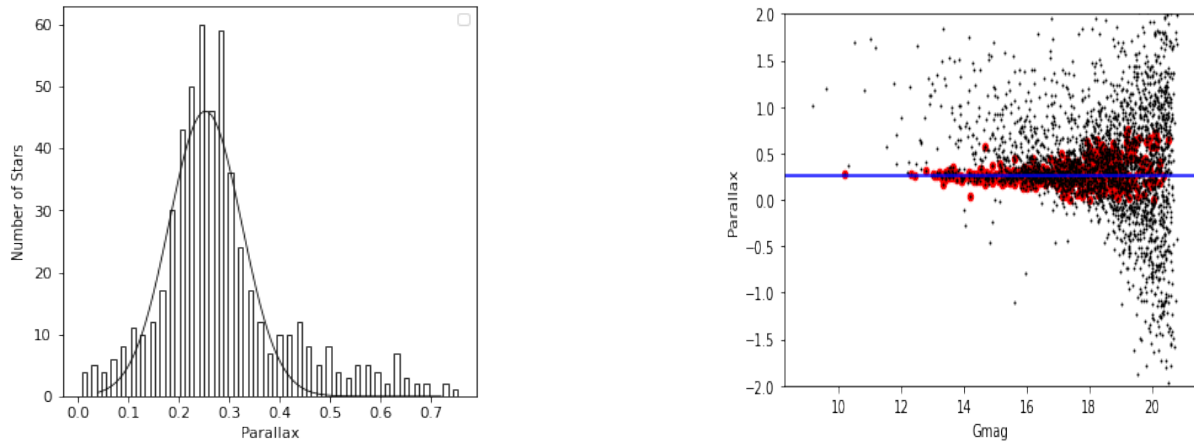


Figure 4.37: Profiles of stellar counts across the region of NGC 2266. a) The Gaussian fits have been applied to the histograms. The center of symmetry about the peaks of R.A. and Dec is taken as the cluster's center. b) The probable member stars with positive parallax are denoted by red in this apparent magnitude vs. parallax graph stars.

red dots denote only positive parallax with membership probability higher than 80 percent, and the black dots are all stars, including the negative parallax.

The blue line drawn at the horizontal center of the probable member strength of this cluster tells us about the mean value that we obtained from Gaussian fitting over constructed histograms of the only positive parallax values of these probable member stars, which also on the visual inspection shows the mean value obtained from the gaussian fitting is completely accurate.

Distance estimation from parallax : Bailer-Jones, 2015 suggested that Gaia has corresponding error values in the parallax data, which can affect the accuracy of distance estimation if determined by inverting the parallax.

The trigonometric parallaxes offer more accurate distance as compared to the other techniques as this technique is not based on the intrinsic properties of the object. The distance obtained from this technique is **3533pc**.

4.3.4 | Radial Density Profile :

To estimate the structural parameters of this cluster, we plotted the radial density profile of this cluster. The mean of Ra, Dec was obtained with Gaussian fitting over histograms of Ra and Dec of only probable members above 80 percent, and it was considered as the center of the cluster for the radial density estimation, and the radius vs. density graph was plotted. The King's profile was fitted into the radial distribution curve to estimate the structural parameters of NGC 2266.

4.3.4.1 | Radial Density Estimation:

Cluster Centre: Ra : 100.832, Dec : 26.976

The cluster center was obtained by fitting two histograms of Ra and Dec for 554 probable members, and by Gaussian fitting; we obtain the mean values of ra, dec as follows:

Mean RA = 100.832 +- 0.005 deg

Mean Dec = 26.976 +- 0.006 deg

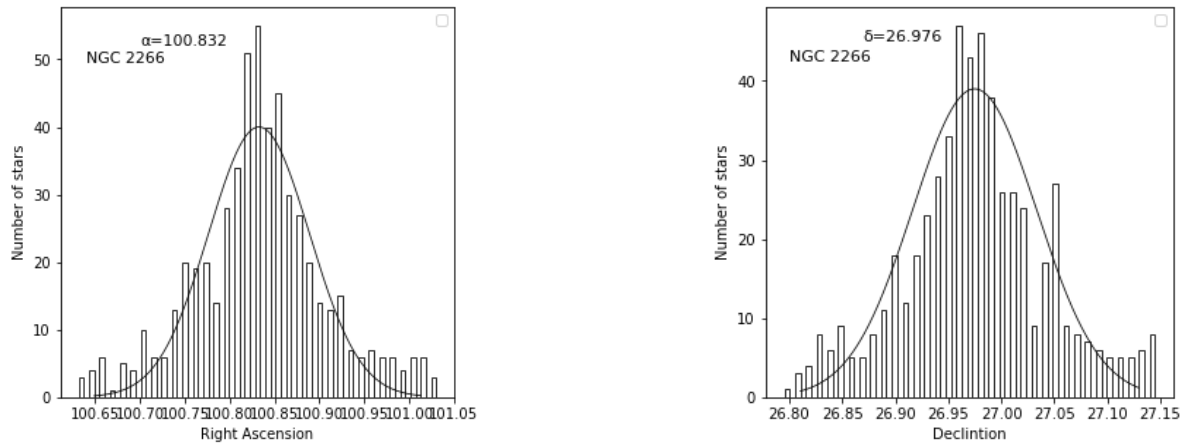


Figure 4.38: Profiles of stellar counts across the region of NGC 2266. The Gaussian fits have been applied to the histograms. The center of symmetry about the peaks of R.A. and Dec is taken as the cluster's center.

Euclidean distance method was used to find the number of stars lying in each circle, considering the mean of RA and DEC to be the center of the cluster, where it was observed as we move away from the cluster's center, the density of stars entrapped per unit area decreases.

The empirical **RDP of King** was also fitted over radial density, and structural parameters were also determined. The variables r , f_{bg} , f_0 , and r_c are the radius from the cluster center, background density, central density, and core radius. The limiting radius can be obtained using the formula and visual inspection.

Another parameter is a density contrast parameter, which was also determined.

The obtained structural parameters are: $r_{lim} = 6'$, $r_c = 1.6'$, $f_{bg} = 0$, $f_0 = 12.95$, contrast = 1.

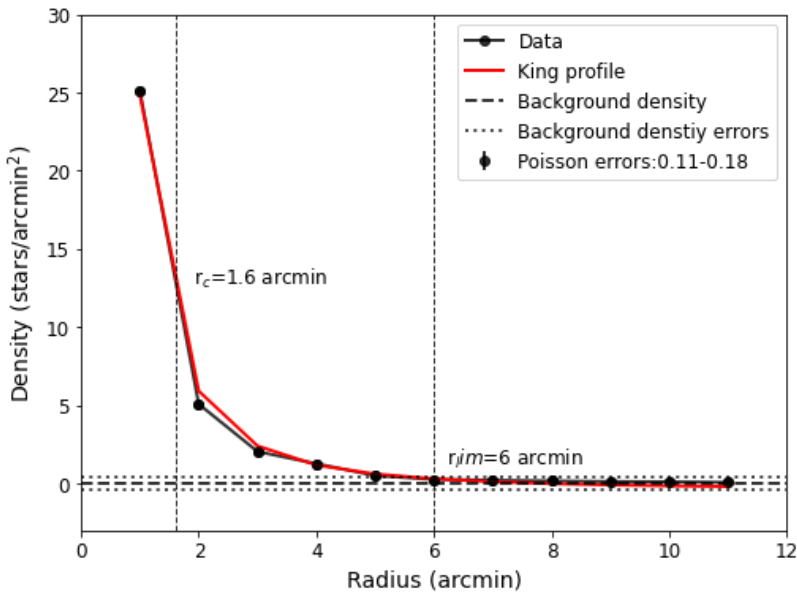


Figure 4.39: Surface Density Distribution of the cluster NGC 2266, where errors are determined using sampling statistics $1 / \sqrt{N}$, where N is the number of stars used in density estimation at that point. The smooth line represents the fitted King's profile, and dashed line represents background density, and the dotted line represents the errors in background density. The Poisson errors are so low in range (0.11– 0.18) that they are not visible in the plot.

4.3.5 | Reddening:

$(J - H)$ versus $(J - K)$ were used in Color Diagrams below to estimate the cluster reddening in the near IR region. The probable members with over 80 percent membership probability were matched with 2mass data. The ZAMS given by Caldwell et al., 1993 fitted on the graph as denoted by a solid line. The dotted ZAMS line denotes the shift in the same ZAMS by the values of $E(J - H)$ and $E(J - K)$. The ratio of $E(J - H)$ and $E(J - K)$ values taken for shifting the ZAMS has to be under 0.55-6.0 mentioned by (Cardelli et al. 1989). The values added to shift the ZAMS are then put in the relations mentioned in (Firoucci & Munari, 2003), and the mean $E(B - V)$ was calculated.

4.3.5.1 | Reddening Estimation:

The matched probable members with 2Mass Photometry JHK data and $J - H$ vs. $J - K$ magnitudes were plotted with 355 probable members. The Caldwell data with $j - h$ and $j - k$ magnitudes is fitted on the graph reaching nearly 0.01 on the y-axis, then a shift is given in the $j - h$ and $j - k$ magnitudes such that it satisfies Cardelli et al.'s ratio, where $\frac{E(J-H)}{E(J-K)} = 0.58$, which shows a good agreement. From here, we have calculated interstellar reddening $E(B - V)$ as 0.17.

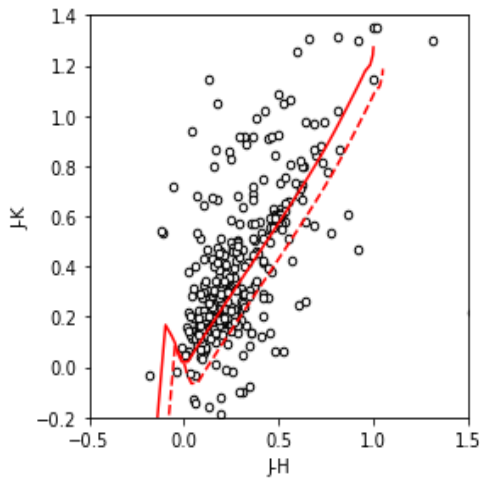


Figure 4.40: **Color Color Diagram:** The red solid line is the zams taken from Caldwell data, where the dotted line is the same zams shifted in such a way that it displaces the solid line.

4.3.6 | Metallicity:

The metallicity of open clusters gives profound information about star formation and evolution for investigating the chemical properties of the galaxy. The mean of metallicities of probable members is transformed to the mass fraction (z) for the selection of isochrones and hence age determination. For the analysis, we used metallicity given in the literature($[z]:= 0.004$).

For the $[\text{Fe}/\text{H}]$ values for NGC 2266, the probable members were matched with the LAMOST dr7 catalog, where with the GMM probable members, metallicities of 64 member stars were obtained, having $z= 0.0084$ and by matching the UPMASK probable members, 25 member stars were obtained with $z=0.0074$.

For the isochrone fitting, the value $z=0.004$ was used.

In the Gaia EDR3, the metallicity values for all the probable member stars are listed, but the metallicity derived from it is very small as compared to the literature; nearly $z=0.00074$ with GMM and $z=0.0009$ with UPMASK because we can not estimate correct metallicity by limited parameters, we have focussed on the z value obtained from the literature.

4.3.7 | Age-Metallicity Relation:

The correct value of metallicity highly corresponds to a good fit. The change in the metallicity value can affect a fit, especially over the main sequence, as shown in the figure.

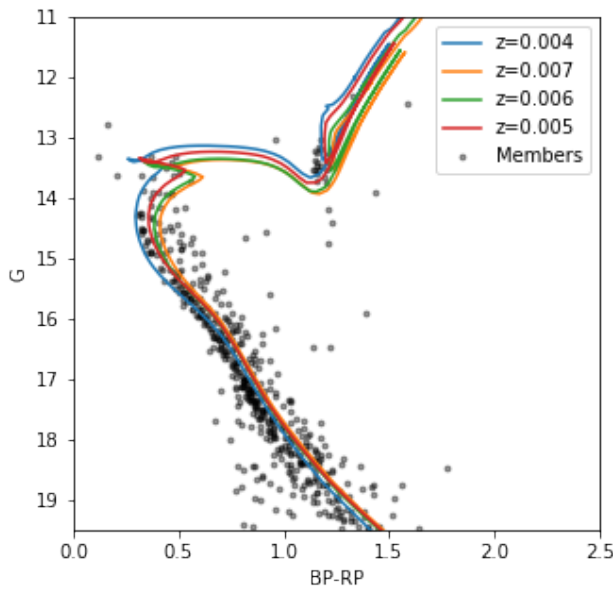


Figure 4.41: The log age 9.05 best-fitted isochrone with different z values to show the importance of correct metallicity.

4.3.8 | Age and Distance Estimation Through Isochrone Fitting :

Color-Magnitude Diagrams were constructed using values for the most probable 545 member stars. This allows for identifying the main sequence, turn-off point, and a group of red giants observed in the NGC 2266. In this study, we estimated the distance moduli and age successfully by fitting Marigo (2017) isochrones to the photometric (GBP - GRP) versus G mag Gaia EDR3 based CMD.

Determination of distance and age: As we tend to fit the isochrone over the main sequence, how much shift we add to the y-axis is called the distance modulus ($m-M$).

The cluster's age through an isochrone fitting can be determined, where the log value of best-fit isochrone is calculated. The unit used for the cluster NGC's age is Gigayear (Gyr).

The distance of the cluster from the sun is 3311 parsec.

The age of cluster NGC 2266 is 0.957 ± 0.02 Gyr, where 0.02 is the uncertainty in age.

The best fit at log age 9.07 can be seen in the figure below.

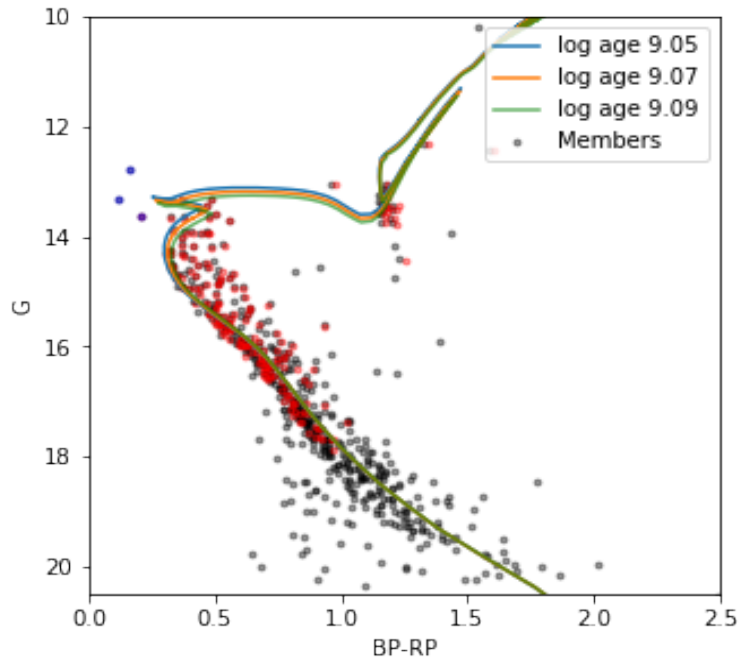
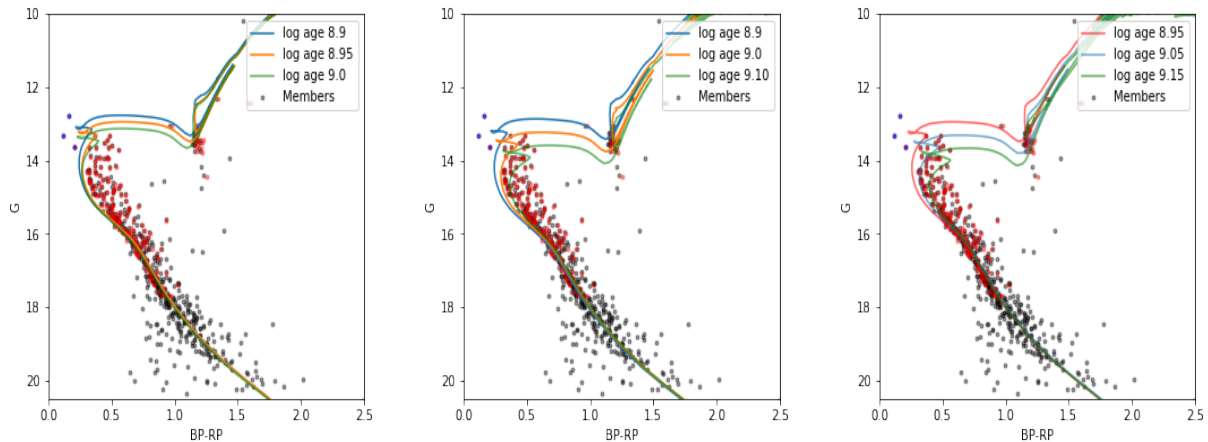


Figure 4.42: All the stars here are probable member stars above 80 percent probability. The curves are isochrones of log ages 8.95, 9.05, and 9.15. The red stars denote 194 probable members matched with Cantat-Gaudin members with above 80 percent membership probability.

4.3.8.1 | Other Isochrone fittings :



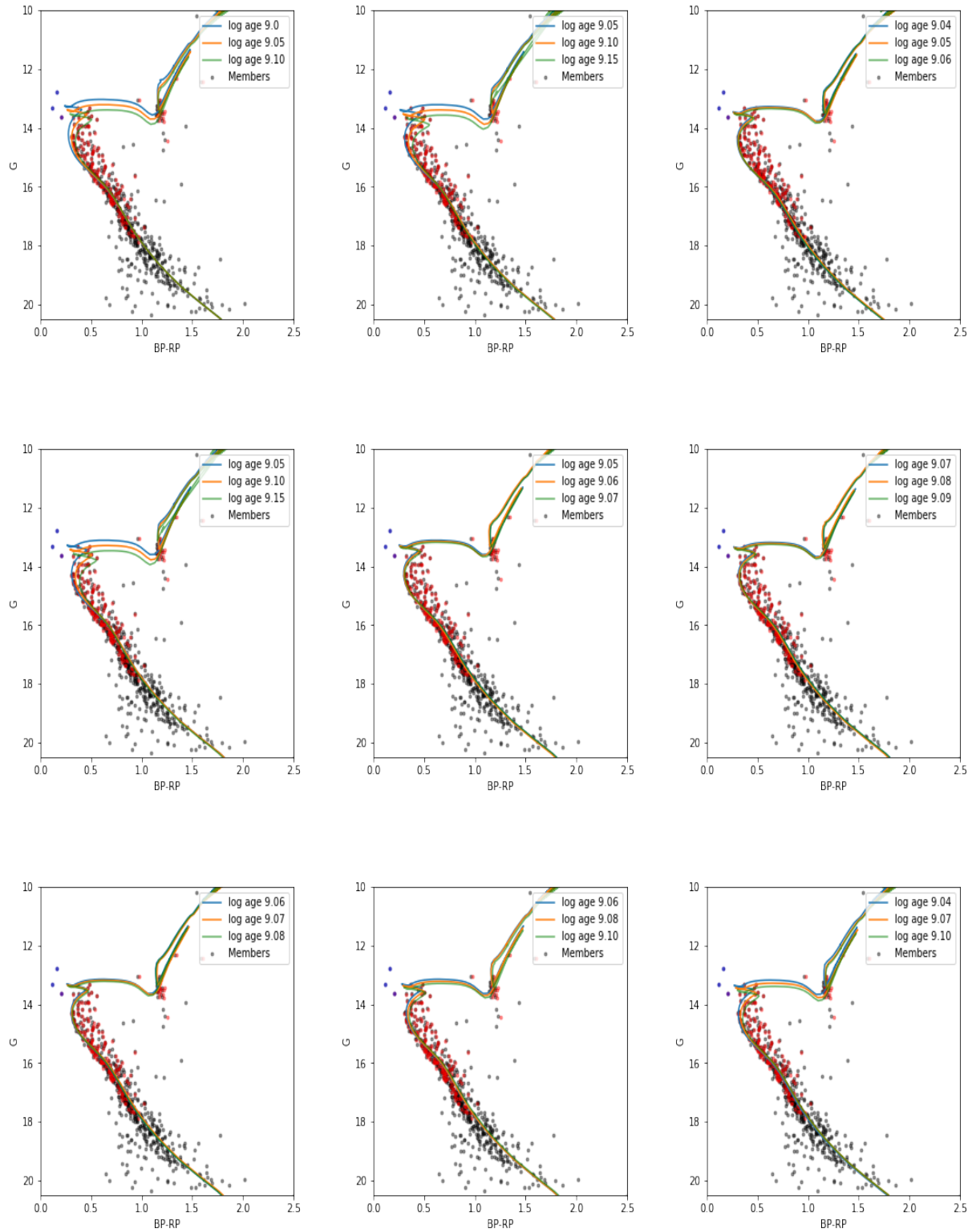


Figure 4.43: Isochrone fittings with different log ages.

4.3.9 | Blue Straggler Stars (BSS):

Blue Stragglers are those stars that are more luminous and bluer than the other stars. These are hot, blue, and massive, having different trajectories of evolution from the turn-off point, visible at 13 mag- 14mag.

Three blue stragglers were observed in the probable members, where one matched with the Cantat Gaudin's probable members having membership probability above 80 percent, as seen in the figure below.

Two blue straggler stars were listed by a paper Antiagecenter-Hyades.

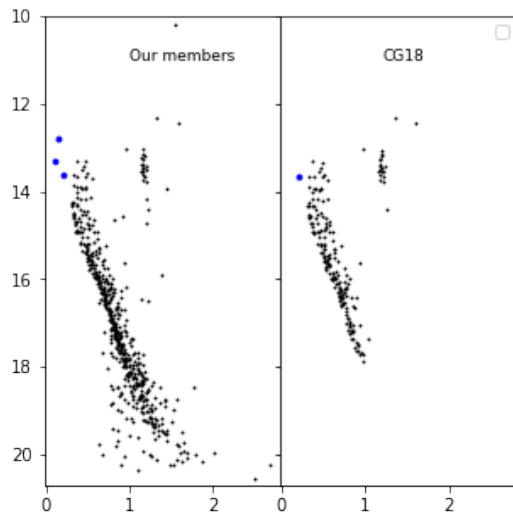


Figure 4.44: The suspected blue straggler stars with blue dots in CMD.

4.3.10 | Luminosity Function :

The luminosity function for an open cluster can be described as the distribution of the main-sequence members in different absolute magnitude ranges. The relative histogram was created with a bin width of 1 mag; the M_v rises maximum to 1mag.

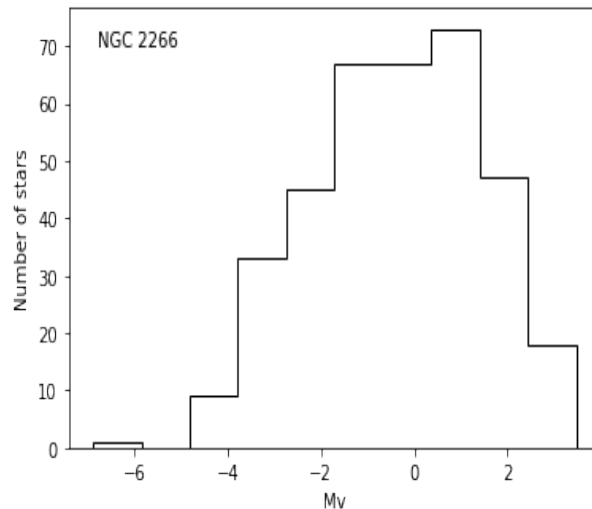


Figure 4.45: Luminosity function of NGC 2266 using members.

4.4 | Result: Berkeley 70

Berkeley 70 is located in a direction toward which many foreground stars are located. The CMDs of the cluster show a broad main sequence due to heavy contamination by field stars. The color-color diagram appears to be complicated due to the field star contamination. The heavy contamination of field stars is apparent from the cleaned CMD of Berkeley 70 in Fig. 4.21. However, some of the bright blue stars above the turnoff point of the main sequence of Be 70 may be blue straggler stars from their presence in the cleaned CMD of the cluster. Owing to the well-developed giant branch and the highly populated main sequences, it is not difficult to fit the isochrones to the stellar distributions in the CMDs.

4.4.1 | Membership Analysis

To determine the membership of the cluster stars, we first extract all the stars within a radius of 0.3 mas/yr in the vector point diagram (VPD). Eye inspection of the VPD determined this initial cut to eliminate most field stars. This is followed by applying the stand-alone code UPMASK (<https://github.com/msolpera/pyUPMASK>). The underlying principle of UPMASK is simple. The code uses a Gaussian mixture model for clustering the input data based on user-defined inputs. We use the proper motion (pmra and pmdec), parallax, and the position of the stars (ra and dec) as inputs to the clustering model. The motivation behind this is that the members of the clusters will share very similar parallax, positions, and proper motions, while any foreground or background star will differ from these values. The clustering algorithm can then easily separate the cluster members from the non-members.

4.4.2 | Physical parameters of the cluster

Once the cluster members are identified, it is possible to obtain the physical parameters of the cluster, such as mean parallax and proper motions. The proper motion in RA is $0.86 \pm 0.04 \text{ mas/yr}$ while the proper motion in declination is $1.84 \pm 0.04 \text{ mas/yr}$. The parallax distribution can't be approximated as a normal distribution since it will then include the negative parallaxes, which are unphysical. We, therefore, use a Gaussian kernel density estimate to fit the distribution of parallaxes and use percentile values for the parallaxes. The 90% percentiles for the parallax value are between 0.185 mas and 0.212 mas.

4.4.3 | Color magnitude diagram

Color-magnitude diagram (CMD) for Berkeley 70 is given below. We can see the distinction between the field and cluster stars from the CMD. We compare the CMD with the one from the

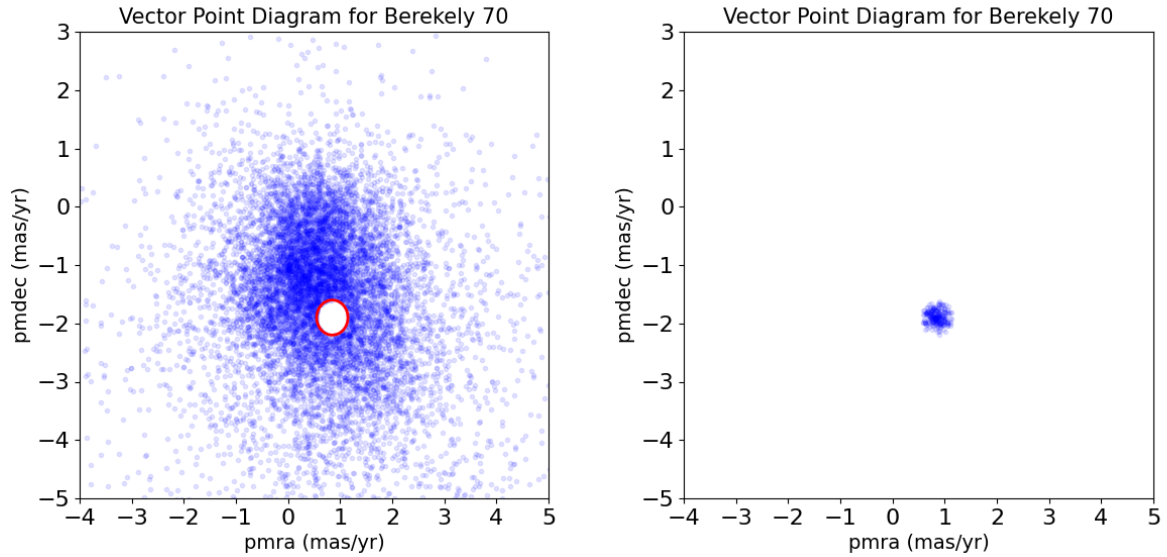


Figure 4.46: An initial cut of 0.3 mas/yr is used to separate the possible cluster stars from the field stars

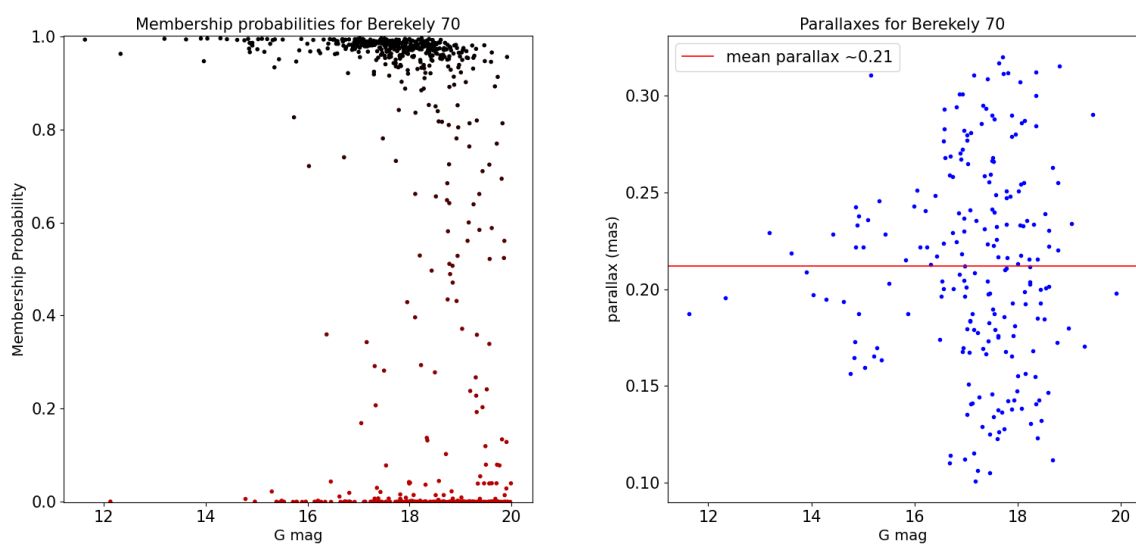


Figure 4.47: Membership probabilities of Berkeley 70

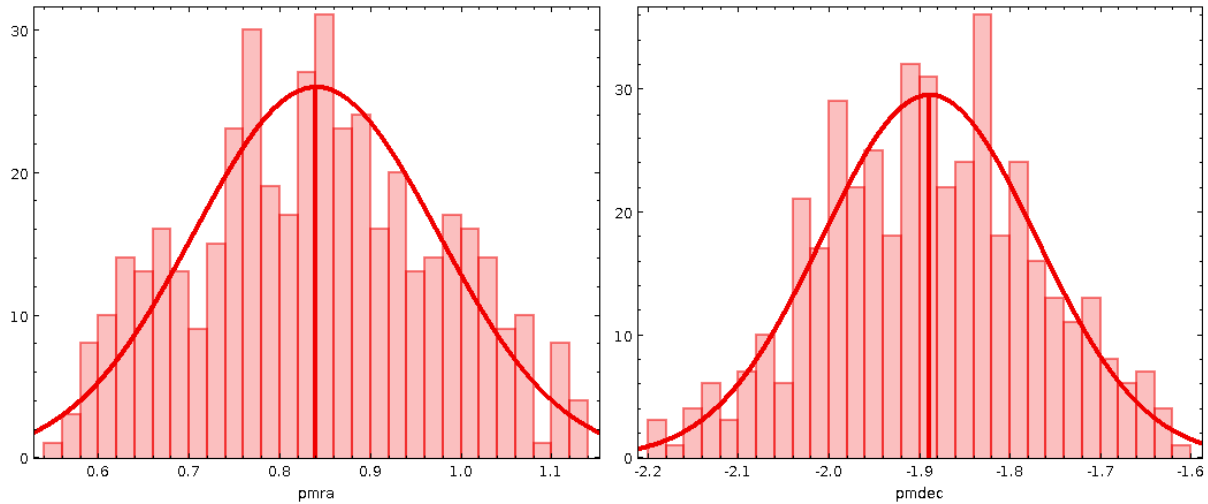


Figure 4.48: Proper motion distribution of Berkeley 70

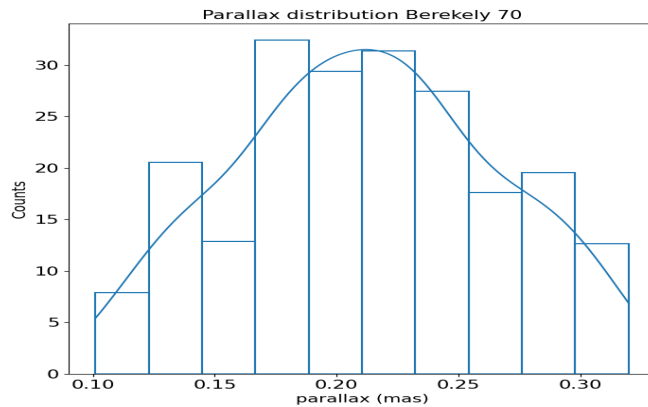


Figure 4.49: Distribution of parallaxes of the cluster Berkeley 70. Here the negative (unphysical) parallaxes are excluded.

catalog of Cantat Gaudin. The cantat-Gaudin catalog includes the stars with a G magnitude of 18 or less, while in this study, we stretch our magnitude limit to 20.

4.4.4 | Extinction

To find the extinction of the cluster, we first look for the 2MASS data using TOPCAT. TOPCAT provides a quick way to cross-match and merge custom catalogs of stars based on their positions. We plot the color-color diagram (j-h versus j-k) to measure the extinction and then fit the Caldwell zero-age main sequence to the data. The best fit gives a value of $E(j-h) =$

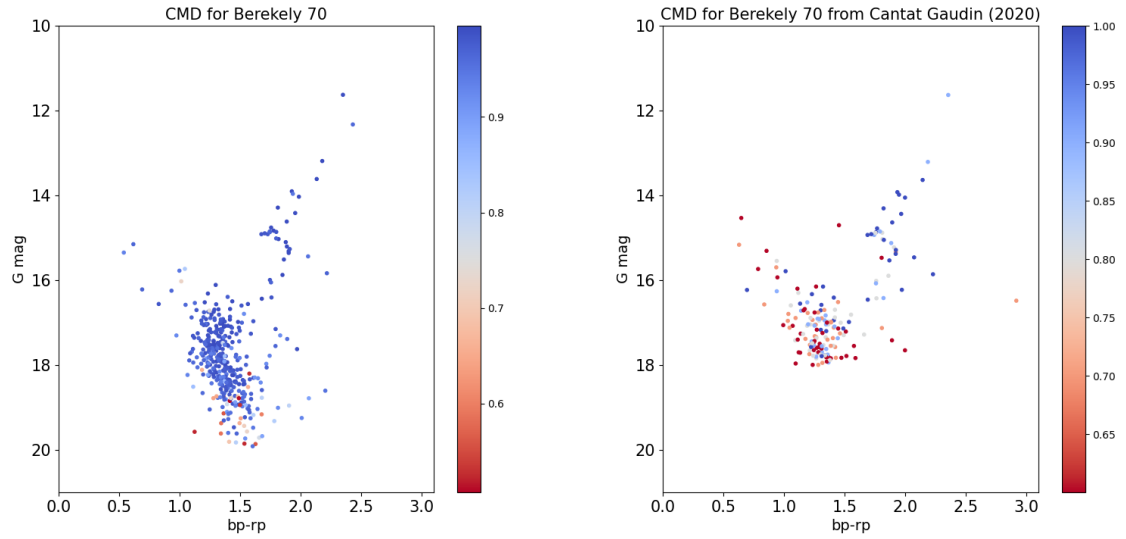


Figure 4.50: Color magnitude diagram for Berkeley 70 with all stars having membership probability larger than 50% (right) and the comparison to the members from a catalog of Cantat-Gaudin (left). The color bar on the right indicates the membership probability.

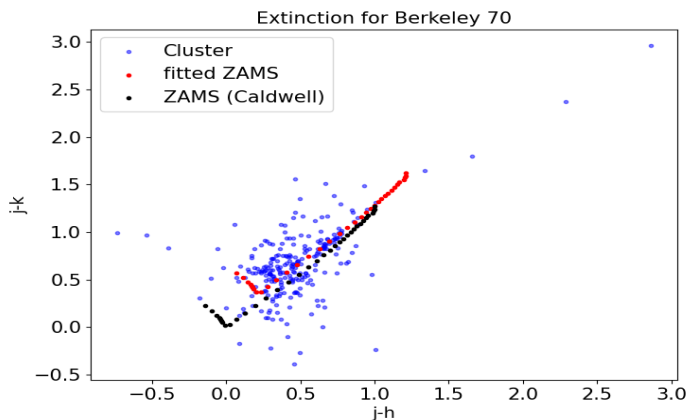


Figure 4.51: Color-color diagram for Berkeley 70 from 2MASS data. Calwell ZAMS is fitted to the data to estimate the extinction.

4.4.5 | Isochrone fitting

Age isochrones are one of the most direct ways of estimating the age of a cluster. In this study, we fit a grid of Padova isochrones to the cluster members. The fitting procedure follows Flannery and Johnson's (1982)'s method. The fitting procedure also uses the membership probabilities as an additional weighting factor. The idea is that a star with a 99% probability of being a cluster member will have more weight in the fitting procedure than a star with a 50%

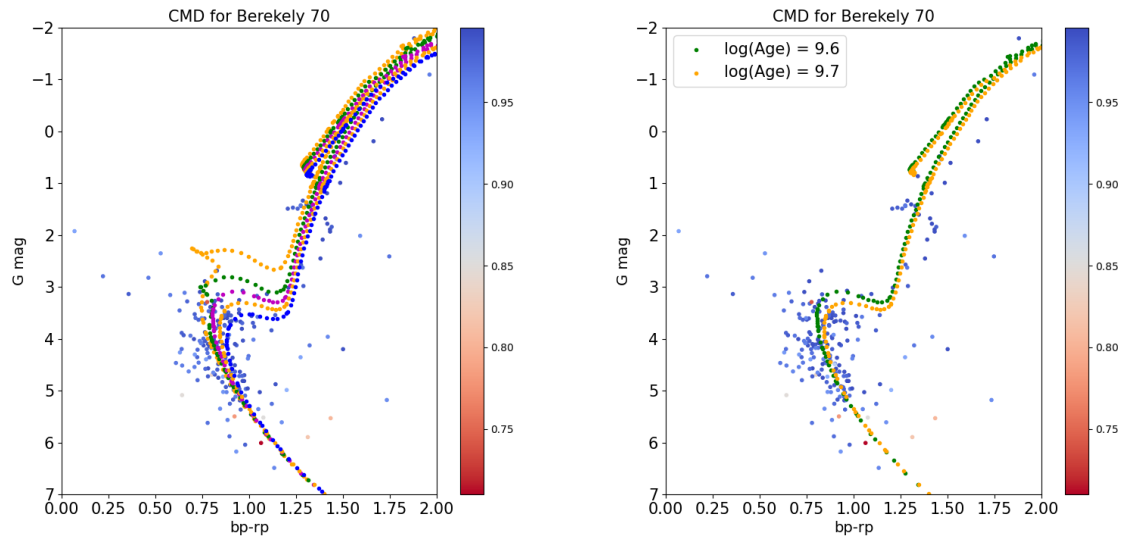


Figure 4.52: Example of the grid of Padova isochrones used to fit the age for Berkeley 70 (right) and the best-fitted isochrone used for age estimation (left)

probability. The best-fitted isochrone gives the cluster's age, which is 3.98 Gyr ($\log \text{Age} = 9.6$).

4.5 | Result: Tombaugh 4

4.5.1 | Membership Analysis and Others

Using the GAIA EDR3 data, we analyzed the results for the old open cluster Tombaugh 4 with pyUPMASK. As previously mentioned, Tombaugh 4 is present in a rich cluster. The GAIA EDR3 data with a search radius of 10 arcmin yielded 4500 stars. After doing the pyUPMASK analysis, built over the original UPMASK package, we isolated 484 stars with a probability above 0.9.

The G-magnitude vs. the probabilities plot of cluster members (in red) and field stars (in black) shows the magnitudes over which the stars in the clusters are situated. The parallax vs. G-mag plot is also given where the solid circles represent cluster member stars above 50% probability. We will only use these cluster members for subsequent studies unless otherwise specified. The parallax measurements have been considered by applying a certain offset to fix

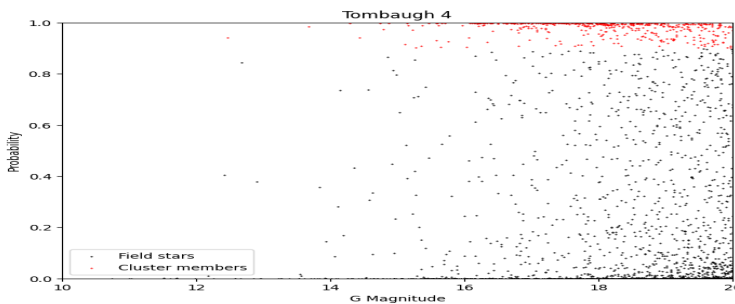


Figure 4.53: G-magnitude vs. Probability of Tombaugh 4

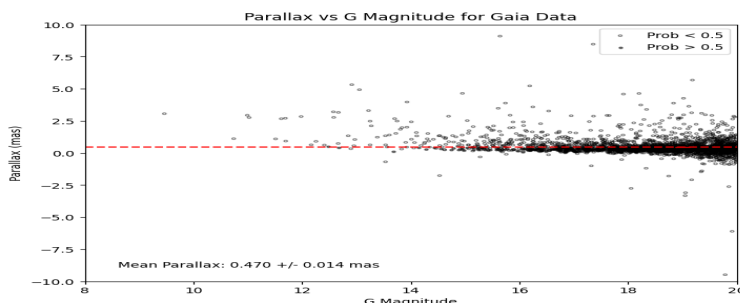


Figure 4.54: G-magnitude vs Parallax for Tombaugh 4

any biased values. The mean parallax value obtained for Tombaugh 4 is 0.470 ± 0.014 mas.

4.5.2 | RA, DEC, and Proper Motion analysis

The obtained coordinates for the cluster center are RA = 37.3 and DEC = 61.78. The mean values for proper motion and its components obtained with Gaussian fitting are: Mean proper motion

in RA = $RA : -0.987 \pm 0.021$ mas/yr, Mean proper motion in DEC: -0.109 ± 0.018 mas/yr
 Further, the VPD, i.e., the Vector Point Diagram, has been plotted, a plot of the pmra vs pmdec

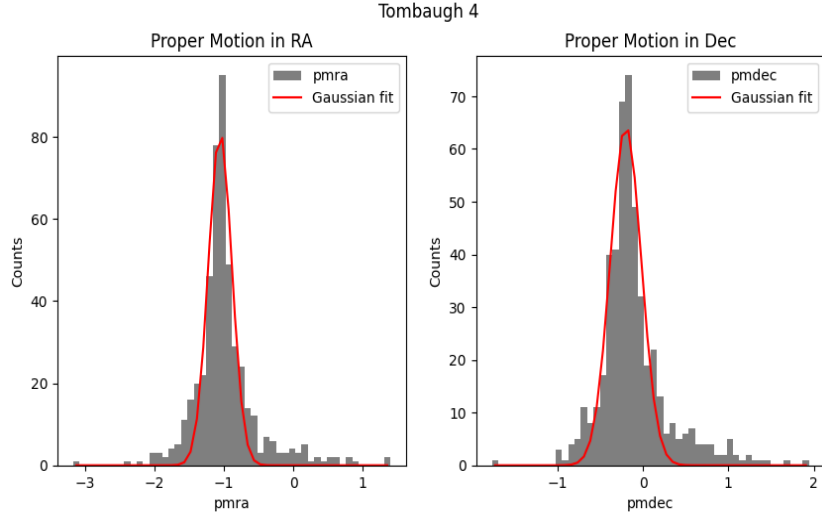


Figure 4.55: Proper motion components vs. the number of counts of Tombaugh 4

where each star in a cluster is represented as a point. In previous studies, it has been used to identify cluster members using all stars, i.e., the field and cluster stars.

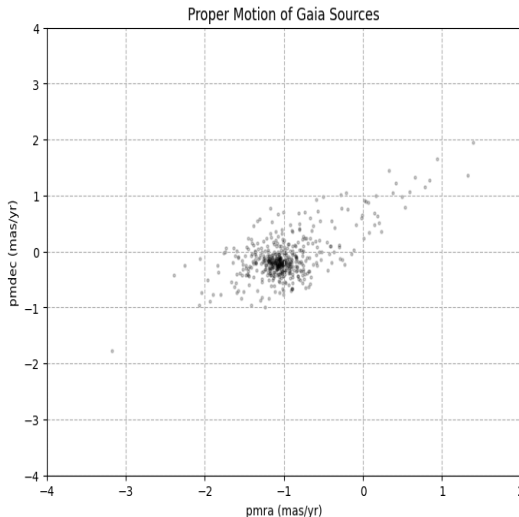


Figure 4.56: Vector Point Diagram of Tombaugh 4

4.5.3 | Color Magnitude Diagram (CMD)

The CMD obtained for Tombaugh 4 is given below. The comparison between the CMD of field stars, cluster stars, and field stars is visible. The region containing all stars and field stars is

heavily crowded, whereas the CMD of cluster stars is clean. A comparison with Cantat-Gaudin Catalogue is also given, which used Gaia DR2 data with a G-magnitude cut-off of 18.

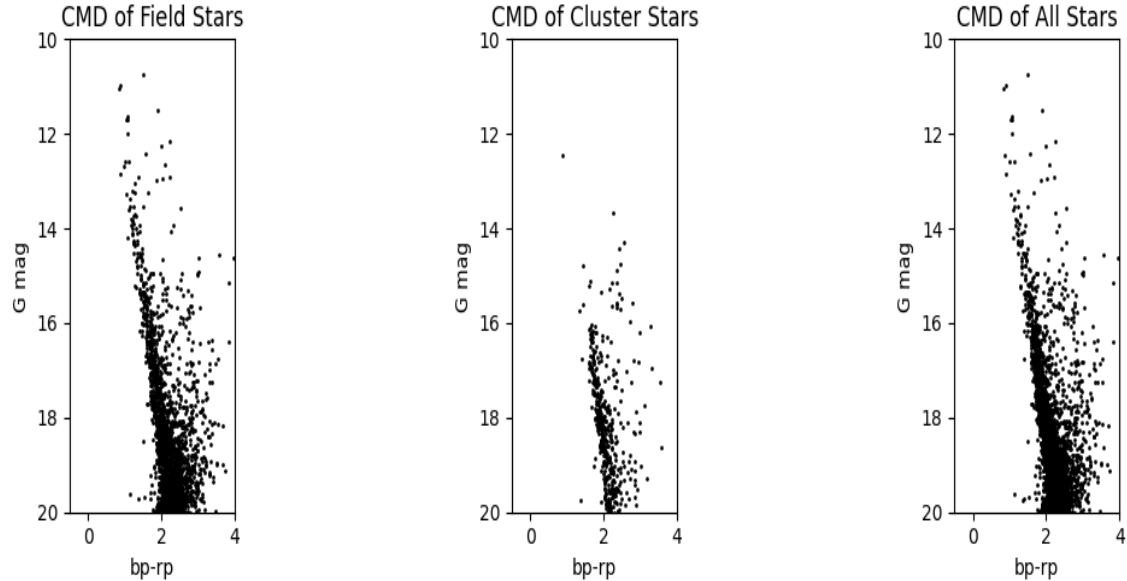


Figure 4.57: CMD of Tombaugh 4

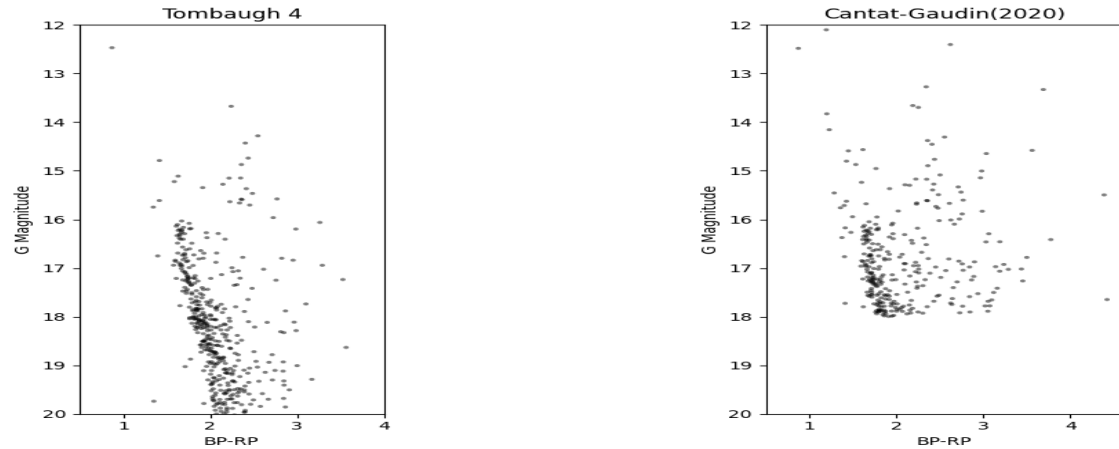


Figure 4.58: Cantat-Gaudin Catalogue(2020) CMD comparison with observed CMD of Tombaugh 4

4.5.4 | Interstellar Reddening

In this study, as previously mentioned, the near-infrared 2MASS data has been utilized to determine $E(B-V) = 1.012 \pm 0.024$. The ratio of $E(J-H)$ and $E(J-K)$ is 0.59, which is in good agreement

with Cardelli et al. (1989). The observed reddening is consistent with the existing literature i.e. Maciejewski and Niedzielski (2007) estimated $E(B-V)$ for Tombaugh 4 = 1.01 ± 0.008 .

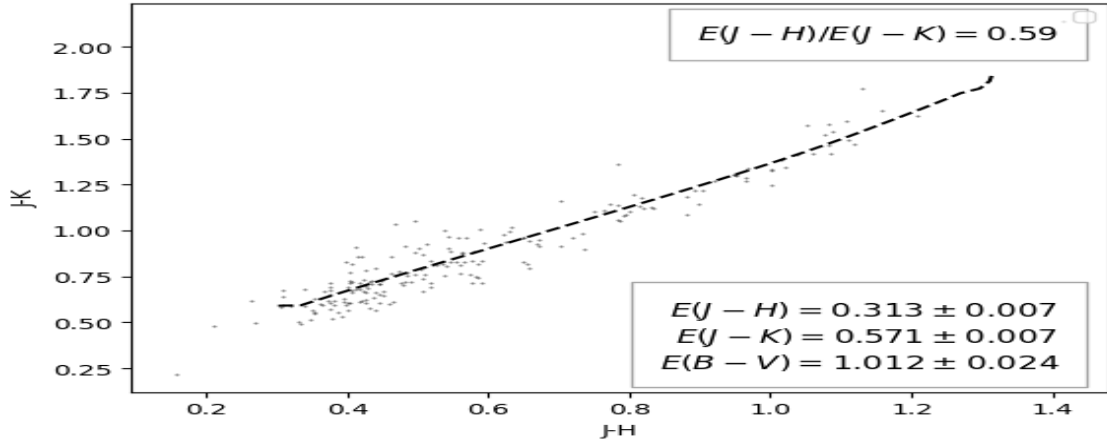


Figure 4.59: Color-color diagram for Tombaugh 4, using 2MASS data

4.5.5 | Isochrone fitting

Using PARSEC isochrones of different ages and fitting them over the observed CMD of Tombaugh 4, obtained $\log(\text{age}) = 9.2$ with metal fraction ' z' ' = 0.009. It can be concluded that the $\log(\text{age}) = 9.15$ and 9.25 are not a good fit for the CMD, whereas $\log(\text{age}) = 9.2$ seems to overlap the MS and giant branch well along with the MSTO.

The potential blue straggler stars (BSS) have been marked as blue solid dots near the MSTO, as these celestial objects are generally found in such regions.

4.5.6 | Luminosity Function (LF)

For the dynamical study of the cluster, the distance modulus is used to obtain the absolute magnitudes of the main sequence stars. We have plotted the histograms of LF with intervals of

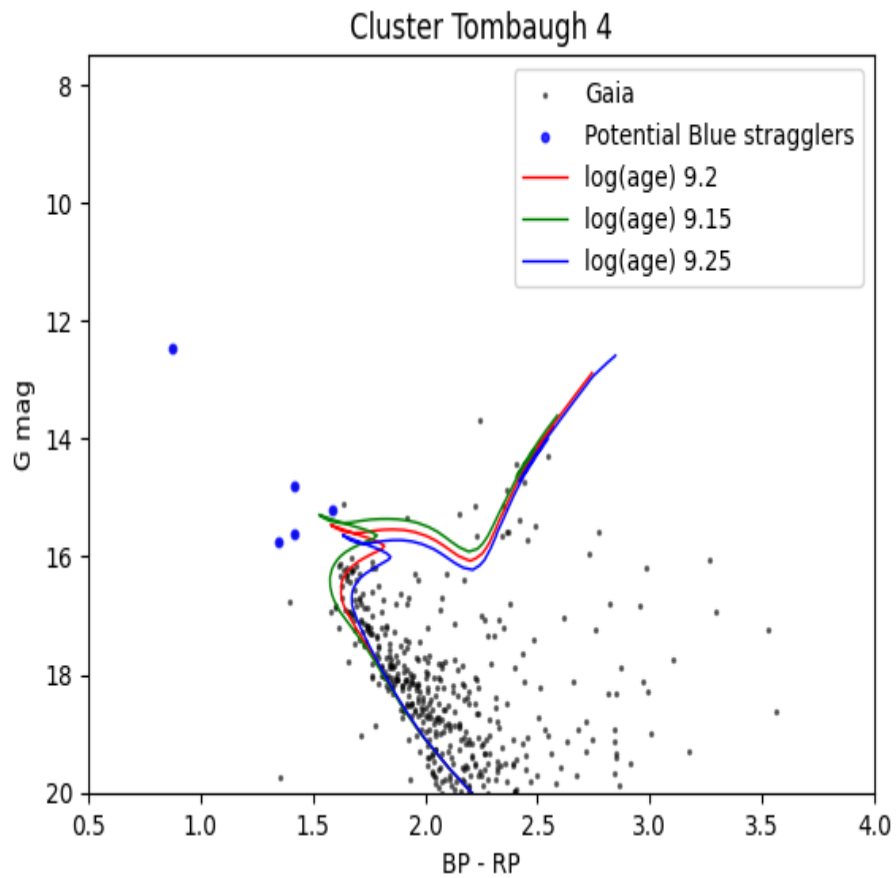


Figure 4.60: Isochrone fitted CMD of Tombaugh 4

1.0 mag. The LF continues to rise to $M(g) = 3.5$ for the cluster. The mean luminosity function value obtained = 3.922 mag.

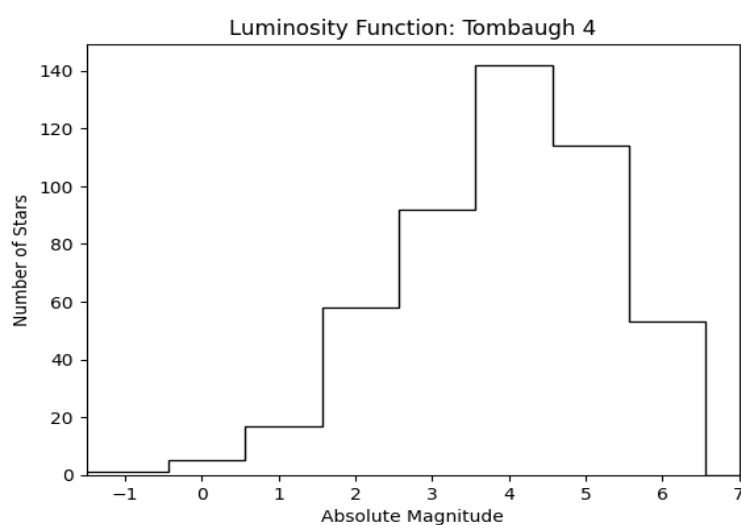


Figure 4.61: Luminosity function of Tombaugh 4

Discussion & Conclusions

5.1 | Berkeley 26

In summary, the analysis of Berkeley 26 involved the identification of cluster members using multidimensional GAIA EDR3 data and utilizing membership probability calculations. The cluster's distinct nearby cluster, Berkeley 27, was taken into account during the analysis. Filtering data based on search radius and membership probability resulted in a subset of stars likely to represent genuine cluster members. Proper motion analysis provided insights into the distribution of cluster members and field stars in space. Gaussian fitting determined the mean values of proper motion in different directions. Interstellar reddening was also obtained for Berkeley 26. A color-magnitude diagram (CMD) was plotted, which allowed for determining the cluster's age, distance, and reddening using theoretical fitting models. The estimated $\log(\text{age})$ and metal fraction were compared to PARSEC isochrones to validate the analysis. Additionally, the presence of blue straggler stars in the cluster was identified.

5.2 | Berkeley 70

In conclusion, the analysis of Berkeley 70 reveals heavy contamination of field stars, which complicates the interpretation of the color-color and color-magnitude diagrams (CMD). However, applying the UPMASK code and membership probability analysis makes it possible to identify the cluster members and separate them from the field stars. The physical parameters of the cluster, such as mean parallax, proper motions, and extinction, are determined, providing valuable information about the cluster's location and motion. The CMD analysis, aided by isochrone fitting, allows for estimating the age of Berkeley 70 as 3.98 Gyr. Despite the challenges of field star contamination, the study successfully characterizes Berkeley 70 and provides insights into its stellar population.

5.3 | Berkeley 45

To verify consistency with the literature, a table with obtained parameters from previous studies and our present study has been given for some of the main parameters. The mean proper

motion and mean parallax values have been discussed in the result section. In the future, the aim is to include other structural and dynamical parameters, such as mass function and galactic orbits. We have estimated a slightly older age for Berkeley 45. The estimated reddening value determined with 2MASS is consistent with Tadross (2010).

Table 5.1: Comparison of the present study with literature for Berkeley 45

References	log(age)	E(B-V)	Distance Modulus (DM)	Photometry
Tadross (2010)	8.77	0.82	12.5	2MASS
Subramaniam et al. (2010)	8.5-8.6	1.4	16.2	BV I CCD
Present study	9	0.80	14.55	GAIA EDR3, 2MASS

5.4 | Tombaugh 4

To conclude our study for the old open cluster Tombaugh 4, a table with certain parameters from the literature and the present study has been shown below. The E(B-V) and obtained distance in parsecs show consistency with the literature. Slightly older age has been obtained with GAIA data. In the future, the plan will include other structural and dynamical parameters for the cluster.

Table 5.2: Comparison of the present study with literature for Tombaugh 4

References	log(age)	E(B-V)	DM	Distance(pc)	Photometry
Maciejewski and Niedzielski (2007)	9	1.01	14.81	2.17	CCD BV
Subramaniam et al. (2010)	8.6-8.7	1.25	16.8	3850	CCD BV
Present study	9.2	1.012	14.4	3775.15	GAIA EDR3, 2MASS

Future Work

6.1 | Scope 1

Under this project, we aim to investigate mass function for all our target clusters. It will help us understand the stellar evolution process and trace the structure of our Milky Way Galaxy.

6.2 | Scope 2

It is planned to determine the orbits of the open clusters using various gravitational potential models. We will use the proper motion and parallax data from the Gaia DR3 database for orbit calculations.

6.3 | Scope 3

We aim to estimate the binary content in those clusters towards core and off-core regions which will be helpful to gather information regarding the dynamical aspects of clusters.

References

- H. B. Ann, S. H. Lee, H. Sung, M. G. Lee, S.-L. Kim, M.-Y. Chun, Y.-B. Jeon, B.-G. Park, and I.-S. Yuk. BOAO photometric survey of galactic open clusters. II. physical parameters of 12 open clusters. *The Astronomical Journal*, 123(2):905–914, February 2002a. doi: 10.1086/338309.
- HB Ann, SH Lee, H Sung, MG Lee, S-L Kim, M-Y Chun, Y-B Jeon, B-G Park, and I-S Yuk. Boao photometric survey of galactic open clusters. ii. physical parameters of 12 open clusters. *The Astronomical Journal*, 123(2):905, 2002b.
- Devendra Bisht, Qingfeng Zhu, Waleed H Elsanhoury, Devesh P Sariya, Geeta Rangwal, Ramakant Singh Yadav, Alok Durgapal, and Ing-Guey Jiang. Detailed analysis of the poorly studied northern open cluster ngc 1348 using multi-color photometry and gaia edr3 astrometry. *Publications of the Astronomical Society of Japan*, 73(3):677–691, 2021.
- John AR Caldwell, AWJ Cousins, CC Ahlers, P Van Wamelen, and EJ Maritz. Statistical relations between the photometric colours of common types of stars in the ubv (ri) c, jhk, and uvby systems. *South African Astronomical Observatory Circular*, 15:1, 1993.
- T Cantat-Gaudin and F Anders. Clusters and mirages: cataloguing stellar aggregates in the milky way. *Astronomy & Astrophysics*, 633:A99, 2020.
- Jason A Cardelli, Geoffrey C Clayton, and John S Mathis. The relationship between infrared, optical, and ultraviolet extinction. *The Astrophysical Journal*, 345:245–256, 1989.
- R Carrera. Radial velocities and metallicities from infrared ca ii triplet spectroscopy of open clusters-berkeley 26, berkeley 70, ngc 1798, and ngc 2266. *Astronomy & Astrophysics*, 544:A109, 2012.
- M Fiorucci and U Munari. The asiago database on photometric systems (adps)-ii. band and reddening parameters. *Astronomy & Astrophysics*, 401(2):781–796, 2003.
- Xiaoting Fu, Angela Bragaglia, Chao Liu, Huawei Zhang, Yan Xu, Ke Wang, Zhi-Yu Zhang, Jing Zhong, Jiang Chang, Lu Li, et al. Lamost meets gaia: The galactic open clusters. *Astronomy & Astrophysics*, 668:A4, 2022.
- Takashi Hasegawa, Hakim L Malasan, Hideyo Kawakita, Hitoshi Obayashi, Tsutomu Kurabayashi, Tatsuji Nakai, Masaaki Hyakkai, and Nobuo Arimoto. New photometric data of old open clusters in the anti-galactic center region. *Publications of the Astronomical Society of Japan*, 56(2):295–311, 2004.
- Takashi Hasegawa, Tsuyoshi Sakamoto, and Hakim Luthfi Malasan. New photometric data of old open clusters ii. a dataset for 36 clusters. *Publications of the Astronomical Society of Japan*, 60(6):1267–1284, 2008a.
- Takashi Hasegawa, Tsuyoshi Sakamoto, and Hakim Luthfi Malasan. New photometric data of old open clusters ii. a dataset for 36 clusters. *Publications of the Astronomical Society of Japan*, 60(6):1267–1284, 2008b.
- Vikrant V Jadhav and Annapurni Subramaniam. Blue straggler stars in open clusters using gaia: dependence on cluster parameters and possible formation pathways. *Monthly Notices of the Royal Astronomical Society*, 507(2):1699–1709, 2021.

- Ivan King. The structure of star clusters. i. an empirical density law. *The Astronomical Journal*, 67:471, 1962.
- G Maciejewski and A Niedzielski. Ccd bv survey of 42 open clusters. *Astronomy & Astrophysics*, 467(3):1065–1074, 2007.
- Paola Marigo, Léo Girardi, Alessandro Bressan, Philip Rosenfield, Bernhard Aringer, Yang Chen, Marco Dussin, Ambra Nanni, Giada Pastorelli, Thaíse S Rodrigues, et al. A new generation of parsec-colibri stellar isochrones including the tp-agb phase. *The Astrophysical Journal*, 835(1):77, 2017.
- H Monteiro, WS Dias, and TC Caetano. Fitting isochrones to open cluster photometric data-a new global optimization tool. *Astronomy & Astrophysics*, 516:A2, 2010.
- María Sol Pera, Gabriel Ignacio Perren, A Moitinho, Hugo Daniel Navone, and Ruben Angel Vazquez. pyupmask: an improved unsupervised clustering algorithm. *Astronomy & Astrophysics*, 650:A109, 2021.
- Andrés E Piatti, Juan J Clariá, and Andrea V Ahumada. New fundamental parameters of the galactic open clusters berkeley 26, czernik 27, melotte 72, ngc 2479 and bh 37. *Monthly Notices of the Royal Astronomical Society*, 402(4): 2720–2734, 2010a.
- Andrés E Piatti, Juan J Clariá, and Andrea V Ahumada. New fundamental parameters of the galactic open clusters berkeley 26, czernik 27, melotte 72, ngc 2479 and bh 37. *Monthly Notices of the Royal Astronomical Society*, 402(4): 2720–2734, 2010b.
- Arumalla BS Reddy, Sunetra Giridhar, and David L Lambert. Comprehensive abundance analysis of red giants in the open clusters ngc 2527, 2682, 2482, 2539, 2335, 2251 and 2266. *Monthly Notices of the Royal Astronomical Society*, 431(4): 3338–3348, 2013.
- A Subramaniam, U Gorti, R Sagar, and HC Bhatt. Probable binary open star clusters in the galaxy. *Astronomy & Astrophysics*, 302(1):86–89, 1995.
- Annapurni Subramaniam, Giovanni Carraro, and Kenneth A Janes. Optical photometry and basic parameters of 10 unstudied open clusters. *Monthly Notices of the Royal Astronomical Society*, 404(3):1385–1395, 2010.
- AL Tadross. Vizier online data catalog: Proper motions and jhk of 24 berkeley clusters (tadross, 2008). *VizieR Online Data Catalog*, pages J–MNRAS, 2010.
- Ashraf Latif Tadross. A catalogue of previously unstudied berkeley clusters. *Monthly Notices of the Royal Astronomical Society*, 389(1):285–291, 2008.